European Journal of Medicinal Chemistry 216 (2021) 113300

Contents lists available at ScienceDirect

European Journal of Medicinal Chemistry

journal homepage: http://www.elsevier.com/locate/ejmech

Design, synthesis and biological evaluation of sulfamoylphenyl-quinazoline derivatives as potential EGFR/CAIX dual inhibitors

Bin Zhang [a, b, 1], Zhikun Liu [a, b, 1], Shengjin Xia [a, b], Qingqing Liu [a, b], Shaohua Gou [a, b, *]

[a] Jiangsu Province Hi-Tech Key Laboratory for Biomedical Research, Southeast University, Nanjing, 211189, China
[b] Pharmaceutical Research Center and School of Chemistry and Chemical Engineering, Southeast University, Nanjing 211189, China

ARTICLE INFO

Article history:
Received 16 December 2020
Received in revised form
10 February 2021
Accepted 15 February 2021
Available online 20 February 2021

Keywords:
Dual-target inhibitors
Sulfamoylphenylquinazoline derivatives
EGFR inhibitors
CAIX inhibitors
Anticancer agents

ABSTRACT

Multi-target, especially dual-target, drug design has become a popular research field for cancer treatment. Development of small molecule dual-target inhibitors through hybridization strategy can provide highly potent and selective anticancer agents. In this study, three series of quinazoline derivatives bearing a benzene-sulfonamide moiety were designed and synthesized as dual EGFR/CAIX inhibitors. All the synthesized compounds were evaluated against epidermoid carcinoma (A431) and non-small cell lung cancer (A549 and H1975) cell lines, which displayed weak to potent anticancer activity. In particular, compound **8v** emerged as the most potent derivative against mutant-type H1975 cells, which exhibited comparable activity to osimertinib. Importantly, **8v** exhibited stronger anti-proliferative activity than osimertinib against H1975 cells under hypoxic condition. Kinase inhibition studies indicated that **8v** showed excellent inhibitory effect on $EGFR^{T790M}$ enzyme, which was 41 times more effective than gefitinib and almost equal to osimertinib. Mechanism studies revealed that **8v** exhibited remarkable CAIX inhibitory effect comparable to acetazolamide and significantly inhibited the expression of p-EGFR as well as its downstream p-AKT and p-ERK in H1975 cells. Notably, **8v** was found to inhibit the expression of CAIX and its upstream HIF-1α in H1975 cells under hypoxic condition. Molecular docking was also performed to gain insights into the ligand-binding interactions of **8v** inside $EGFR^{WT}$, $EGFR^{T790M}$ and CAIX binding sites.

1. Introduction

It is currently well-known that most cancers can quickly develop resistance against any single protein or kinase inhibitor [1]. Despite drug combination therapies are used as an alternative approach to achieve efficacy, their benefits are often negated by adverse drug-drug interactions, poor patient compliance, unpredictable pharmacokinetics (PK) and safety profiles [2]. Dual-target anticancer agents have been developed successfully since the beginning of modern pharmacology, and their dual-target properties have contributed to their clinical transformation [3]. Dual-target drugs help to target different biological receptors with the expectation of synergistic effects and address the limited efficacy and resistance or toxicity associated with many single-target or combination-based therapies [4]. A rational design to discover dual-target agents is established based on some pharmacophores that are maintained and another is introduced to yield hybrid molecules [4a].

Epidermal growth factor receptor (EGFR), as a transmembrane-bound molecule, has important regulatory functions in cell proliferation, apoptosis, migration, differentiation, and survival [5]. Increased EGFR activity resulting from overexpression, mutation, or amplification of EGFR gene contributes to many human malignancies, including glioblastoma, epithelial cancers of the head and neck, esophagus cancers, breast cancers, and lung cancers, especially in non-small-cell lung cancers (NSCLCs) [6]. Accordingly, interruption of the signaling pathway of EGFR, either extracellularly by blocking the binding site of EGFR or intracellularly by inhibiting the tyrosine kinase activity, is important in cancer prevention and treatment [7]. First-generation (e.g., gefitinib or erlotinib) and second-generation (e.g., afatinib or dacomitinib) quinazoline-based EGFR tyrosine kinase inhibitors (TKIs) (Fig. 1) have remarkably improved survival in advanced EGFR mutant NSCLC patients [1b,8]. However, the emergence of acquired point mutations, particularly

* Corresponding author. Jiangsu Province Hi-Tech Key Laboratory for Biomedical Research, Southeast University, Nanjing, 211189, China.
E-mail address: 2219265800@qq.com (S. Gou).
[1] These authors contributed equally to this work.

https://doi.org/10.1016/j.ejmech.2021.113300
0223-5234/

Abbreviations

EGFR	Epidermal growth factor receptor
TKIs	Tyrosine kinase inhibitors
CAIX	Carbonic anhydrase IX
HIF-1α	Hypoxia inducible factor-1α
ERK	Extracellular signal-regulated kinase
AKT	Protein kinase B
DMF-DMA	*N*,*N*-Dimethylformamide dimethyl acetal
DMF	*N*,*N*-Dimethylformamide;
IC_{50}	Half-maximum inhibitory concentration

T790 M mutation, has weakened their therapeutic efficacy, leading to drug resistance [9]. Thus, the third-generation EGFR covalent inhibitors (e.g., osimertinib or rociletinib) targeting T790 M mutation have been developed [10]. Unfortunately, C797S point mutation and/or other mechanisms have been shown to be associated with the acquired resistance to the third-generation EGFR TKIs [11]. Subsequently, the fourth-generation EGFR TKIs such as EAI045 and other noncovalent inhibitors are being developed to be a major breakthrough against these tertiary mutations [12]. Even so, there is still an unmet medical need to develop novel small molecule inhibitors or therapeutic approaches to overcome multipoint mutations of EGFR.

Oxygen supply is crucial for the growth of cells and is often diminished in solid tumors, especially at the center of the tumor mass, as tumor cells grow faster than the endothelial cells that are crucial for the formation of blood vessels [13]. Tumor cells within hypoxic regions contribute to increased invasion, metastatic spread and therapy resistance [14]. Hypoxia can regulate the expression of several genes, including that encoding carbonic anhydrase IX (CAIX), through binding of the hypoxia inducible factor HIF-1α to a hypoxia-responsive element in the gene. Membrane-bound CAIX contributes to acidification of the tumor environment by efficiently catalyzing the hydration of carbon dioxide to bicarbonate and protons, thereby leading to acquisition of metastatic phenotypes and chemoresistance to weakly basic anticancer drugs [15]. Therefore, many efforts have been made to generate effective CAIX inhibitors as antitumor therapeutics. Recently, the relationship between hypoxia-mediated gene transcription (such as HIF-1α and CAIX) and EGFR expression in hypoxic cells has been reported [16]. Studies suggested that EGFR signaling enhances the cellular response to hypoxia and acts as a survival factor [17]. Thus, the inhibition of hypoxia-mediated gene transcription may provide an attractive treatment strategy for overcoming the tumor resistance of EGFR TKI.

In the current medical era, quinazoline is one of the most important heterocyclic scaffolds in cancer drug discovery and forms a large array of EGFR inhibitors (Fig. 1) [18]. Besides, sulfonamide is a privileged scaffold that is well known for its anticancer activity by many mechanisms such as cyclin-dependent kinase (CDK) inhibition, matrix metalloproteinase (MMP) inhibition and carbonic anhydrase (CA) inhibition (Fig. 1) [19].

Herein we report the synthesis and cytotoxic evaluation of a number of new quinazoline derivatives containing substituted anilide as well as sulfamoylphenyl fragments as EGFR/CAIX dual-target inhibitors. The cytotoxicity of the target compounds was evaluated against three cancer cell lines (human epidermoid carcinoma (A431) and non-small cell lung cancer cells (A549 and H1975)) by MTT assay. Besides, the most active members were examined for their EGFR ($EGFR^{WT}$ and $EGFR^{T790M}$) and CA (CAII and CAIX) inhibitory activity. These compounds elicit potent inhibition of $EGFR^{T790M}$ and CAIX in biochemical settings that translates nicely into improved activity on pertinent NSCLC cell lines. Molecular docking of the promising compound was performed inside the binding site of $EGFR^{WT}$, $EGFR^{T790M}$ and CAIX to gain insights into the molecular interactions and possible modes of action.

2. Results and discussion

2.1. Chemistry

The structures and preparation of target compounds **8a-w**, **15a-n** and **18a-n** are described in Schemes 1 and 2. In Scheme 1, compounds **8a-w** containing 6-hydroxyl-7-methoxy-4-arylaminoquinazoline frameworks (**4a-w**) equipped with specific sulfamoylphenyl warheads were obtained by a substitution reaction of the 6-hydroxyl group with 5-bromo-*N*-(4-sulfamoylphenyl)pentanamide (**7**). The

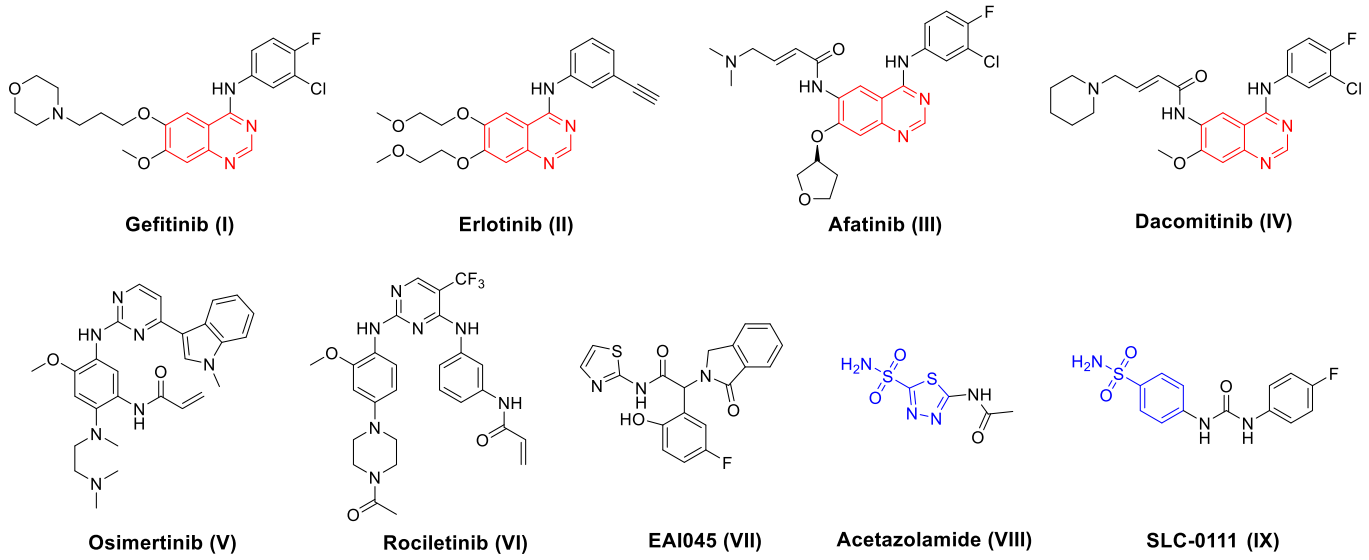

Fig. 1. Chemical structures of selected EGFR inhibitors (**I-VII**) and CA inhibitors (**VIII** and **IX**).

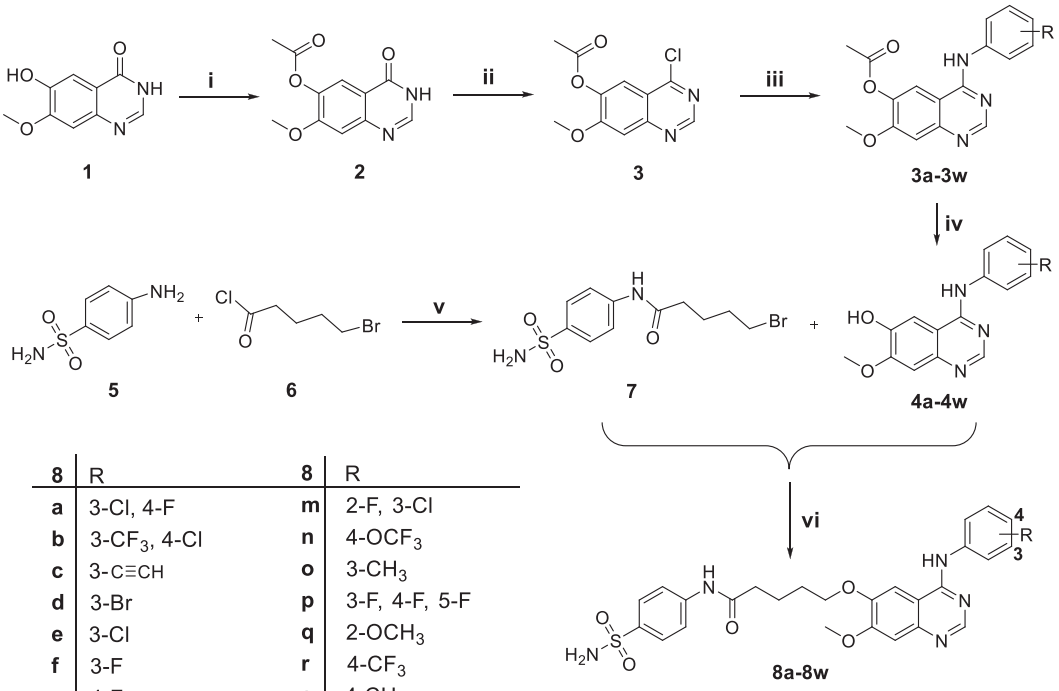

8	R	8	R
a	3-Cl, 4-F	m	2-F, 3-Cl
b	3-CF_3, 4-Cl	n	4-OCF_3
c	3-C≡CH	o	3-CH_3
d	3-Br	p	3-F, 4-F, 5-F
e	3-Cl	q	2-OCH_3
f	3-F	r	4-CF_3
g	4-F	s	4-CH_3
h	4-Cl	t	4-CH_2CH_3
i	4-Br	u	-
j	4-OCH_3	v	3-CF_3
k	3-OCH_3, 4-OCH_3	w	3-Cl, 4-O- 
l	3-Br, 4-F		

Scheme 1. General procedures of preparing compounds 8a-8w.[11] **Reagents and conditions:** (i) $(CH_3CO)_2O$, pyridine, reflux; (ii) $SOCl_2$, DMF, reflux; (iii) substituted aniline, CH_3CN, reflux; (iv) $NH_3 \cdot H_2O$, CH_3OH, reflux; (v) pyridine, DMF, rt; (vi) K_2CO_3, DMF, KI.

synthesis of the anilinoquinazoline scaffold **4a-w** was performed as previously reported with minor adaptations [20]. Compound **7** was obtained by means of acylation of benzenesulfonamide with 5-bromopentanoyl chloride (**6**) in DMF. In Scheme 2, intermediates **12a-n** were synthesized by reacting 5-nitroanthranilonitrile (**9**) with DMF-DMA to afford intermediate **10**, which cyclized upon reaction with different anilines in refluxing glacial acetic acid into 6-nitro-4-anilinoquinazolines **11a-n** through Dimroth rearrangement. Reduction of the latter using Fe/NH_4Cl mixture afforded 6-amino-4-anilinoquinazolines **12a-n**, which were subsequently treated with compounds **14** or **17** in DMF at 60 °C overnight to produce the target compounds **15a-n** and **18a-n**. 4-Isothiocyanatobenzenesulfonamide (**14**) was prepared by reaction of 4-aminobenzenesulfonamide with thiophosgene in water containing concentrated hydrochloric acid [21]. Isothiocyanate **17** was obtained by treated 4-(2-aminoethyl) benzenesulfonamide with dicyclohexylcarbodiimide and carbon disulfide in THF at room temperature. The purities of all compounds were evaluated by HPLC (each compound > 95%). Their structures were characterized by HR-MS and ^1H and ^{13}C NMR spectrometry.

2.2. Antiproliferative activity assay

The antiproliferation activity of the target compounds against human epidermoid carcinoma cells (A431) and non-small cell lung cancer cells (A549 and H1975) were evaluated by MTT assay. A431 and A549 cells have overexpressed $EGFR^{WT}$, while H1975 cells harbor $EGFR^{L858R/T790M}$ mutation [20a,22]. Three commercially available drugs (gefitinib, erlotinib and osimertinib) were used in this test as positive controls.

As shown in Table 1, the obtained results revealed that most of the synthesized compounds showed weak to potent antiproliferative activities against the tested cell lines. For the activity against the wild-type non-small cell lung cancer cell line (A549), compounds **8a**, **8b**, **8c**, **8d**, **8e**, **8m**, **8r**, **8t**, **8v** and **8w** were found to be more potent than gefitinib (IC_{50} = 15.59 μM) and erlotinib (IC_{50} = 16.43 μM) with IC_{50} values ranging from 6.54 to 15.53 μM, while the other compounds had equally or less potent activity than gefitinib and erlotinib. For the wild-type human epidermoid carcinoma cell line (A431), compounds **8a**, **8b**, **8h**, **8i**, **8l**, **8m**, **8o**, **8t**, **8v** and **8w** exhibited effective cytotoxic activities against A431 cell line with IC_{50} values ranging from 3.91 to 8.02 μM, which were more potent than gefitinib (IC_{50} = 8.37 μM). Notably, compounds **8a**, **8b** and **8v** showed stronger cytotoxic activity than osimertinib (IC_{50} = 5.32 μM). For the activity against the mutant-type non-small cell lung cancer cell line (H1975), compounds **8b, 8k, 8m, 8n, 8q, 8t, 8v** and **8w** showed potent activity against H1975 cell line with IC_{50} values ranging from 1.94 to 10.34 μM, which were more active than gefitinib (IC_{50} = 10.78 μM), but all the target compounds had weaker activity against H1975 cell line than osimertinib (IC_{50} = 0.98 μM). Observing the results of antiproliferative tests, we found that benzene sulfonamide substituted for morpholine could contribute to increasing inhibitory effects. Moreover, better antitumor activities presented when 3-positon of the aryl group was occupied with a trifluoromethyl group. More importantly, **8v** had a

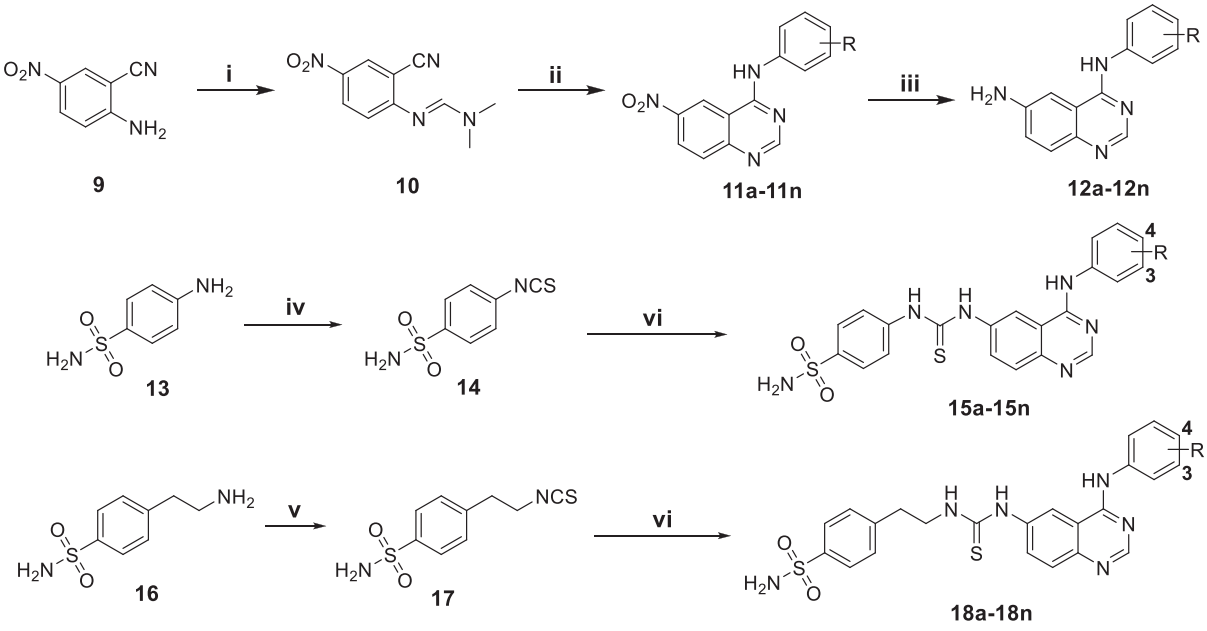

15	R	15	R	18	R	18	R
a	3-Cl, 4-F	h	2-F, 3-Cl	a	3-Cl, 4-F	h	2-F, 3-Cl
b	3-C≡CH	i	3-F	b	3-C≡CH	i	3-F
c	3-CF_3	j	3-Cl	c	3-CF_3	j	3-Cl
d	3-CF_3, 4-Cl	k	3-CH_3	d	3-CF_3, 4-Cl	k	3-CH_3
e	3-Br, 4-F	l	4-CH_3	e	3-Br, 4-F	l	4-CH_3
f	3-Br	m	4-CH_2CH_3	f	3-Br	m	4-CH_2CH_3
g	4-CF_3	n	3-Cl, 4-O-F	g	4-CF_3	n	3-Cl, 4-O-F

Scheme 2. General procedures of preparing compounds 15a-15n and 18a-18n.[11]Reagents and conditions: (i) DMF-DMA, reflux; (ii) substituted aniline, glacial acetic acid, reflux; (iii) Fe, NH_4Cl, EtOH/H_2O (70%), reflux; (iv) hydrochloric acid, thiophosgen, H_2O; (v) DCC, CS_2, THF; (vi) 12a-n, DMF.

comparable anti-tumor activity to osimertinib towards H1975 cell line.

Encouraged by the increased anti-tumor activity of 4-aminoquinazoline derivatives that contain benzene sulfonamide, we further explored the anti-proliferation efficacy of more compounds with the same pharmacophores. As shown in Table 2, compounds **15c**, **15d**, **15f**, **15i**, **15l** and **15m** displayed moderate activity against A549 cells with IC_{50} values range from 2.84 to 25.88 μM. Whereas, these compounds had less activity than gefitinib towards A431 cell line. For the activity against the mutant-type non-small cell lung cancer cell line (H1975), compound **15c** with a trifluoromethyl group in 3-position of the aryl skeleton showed the most potent activity against H1975 cell line, whose IC_{50} value was less than that of gefitinib, but much greater than that of osimertinib.

In order to further explore the effect of increasing carbon chain length on the antiproliferative activity of the compounds, the cytotoxicity of **18a-n** was tested. As described in Table 3, most of compounds exhibited stronger antiproliferative activity towards A549 than gefitinib, with IC_{50} values range from 2.77 to 32.36 μM, which may be attributed to the increase of carbon chain enhancing the lipid solubility of the compound. In addition, compounds **18h** and **18n** displayed effective cytotoxic activities against A431 cell line with IC_{50} values 4.21 and 5.77 μM, which were stronger than gefitinib but almost equal to osimertinib. Moreover, compounds **18c**, **18e**, **18f**, **18l**, **18m** and **18n** possessed effective cytotoxic activities against H1975 cells with IC_{50} values ranging from 4.25 to 10.76 μM, more potent than gefitinib. Among this series compounds, compound **18c** with a trifluoromethyl group in the 3-position of the aryl unit also showed the best anti-tumor activity against H1975 cell line.

The cytotoxic effect of the target compound **8v** was also examined towards normal human liver cells LO2 to investigate the toxicity of the prepared anticancer agent, using gefitinib and osimertinib as positive controls. As shown in Table S1, gefitinib displayed mild cytotoxic effect (IC_{50} value = 33.17 μM), while **8v** and osimertinib hardly have cytotoxicity (IC_{50} value > 40 μM), indicating their relative safety towards normal human liver cells.

2.3. Kinase inhibition study of $EGFR^{WT}$ and $EGFR^{T790M}$

The inhibitory activity of the selected compounds against $EGFR^{WT}$ and $EGFR^{T790M}$ were evaluated using a well-established HTRF KinEASE-TK assay, with gefitinib and osimertinib as positive controls. As shown in Table 4, most of the tested compounds exhibited moderate inhibitory activities against $EGFR^{WT}$ (with IC_{50} 13.7−51.2 nM), in which **8b** and **8w** suppressed $EGFR^{WT}$ more potently than gefitinib. For mutant EGFR, all the tested compounds exhibited better inhibitory activities than gefitinib. Notably, **8v** showed excellent inhibitory effect on $EGFR^{T790M}$, with an IC_{50} value of 9.2 nM, which was 41 times as effective as gefitinib. More importantly, **8v** showed comparable $EGFR^{T790M}$ inhibitory activity

Table 1
In vitro antitumor activity of **8a**-**8v** against different cancer cell lines.

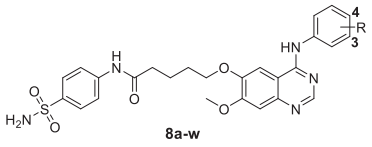

8a-w

Compounds	R	IC_{50} (μM)[a]		
		A549	A431	H1975
8a	3-Cl, 4-F	15.53 ± 0.82	5.02 ± 0.34	35.59 ± 3.45
8b	3-CF_3, 4-Cl	9.27 ± 0.94	3.91 ± 0.23	3.22 ± 0.27
8c	3 − *C≡CH*	7.72 ± 0.25	17.69 ± 0.94	18.75 ± 1.67
8d	3-Br	14.91 ± 0.78	9.75 ± 0.67	11.37 ± 1.09
8e	3-Cl	11.15 ± 0.88	30.38 ± 2.34	33.18 ± 3.12
8f	3-F	>40	29.89 ± 1.89	>40
8g	4-F	>40	18.60 ± 1.23	>40
8h	4-Cl	>40	7.12 ± 0.27	31.78 ± 2.98
8i	4-Br	>40	6.57 ± 0.45	23.29 ± 2.19
8j	4-OCH_3	>40	14.71 ± 0.98	30.19 ± 2.90
8k	3-OCH_3, 4-OCH_3	>40	35.44 ± 2.56	9.23 ± 0.87
8l	3-Br, 4-F	16.02 ± 1.05	8.02 ± 0.47	31.57 ± 2.89
8 m	2-F, 3-Cl	10.46 ± 0.89	5.56 ± 0.23	6.93 ± 0.67
8n	4-OCF_3	>40	22.45 ± 1.56	8.77 ± 0.76
8°	3-CH_3	16.03 ± 0.97	7.46 ± 0.38	32.09 ± 2.79
8p	3-F, 4-F, 5-F	>40	23.41 ± 1.89	19.96 ± 1.89
8q	2-OCH_3	24.05 ± 1.93	24.20 ± 2.12	8.03 ± 0.78
8r	4-CF_3	14.75 ± 1.08	16.88 ± 1.36	11.98 ± 1.12
8s	4-CH_3	>40	35.49 ± 2.67	19.25 ± 1.79
8t	4-CH_2CH_3	12.14 ± 0.83	7.22 ± 0.49	10.34 ± 0.98
8u	–	>40	25.21 ± 2.12	14.10 ± 1.34
8v	3-CF_3	6.54 ± 0.59	4.04 ± 0.34	1.94 ± 0.14
8w	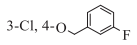	7.86 ± 0.20	7.79 ± 0.45	5.67 ± 0.46
Gefitinib		15.59 ± 1.03	8.37 ± 0.46	10.78 ± 0.45
Erlotinib		16.43 ± 0.96	11.85 ± 0.69	13.12 ± 0.97
Osimertinib		–	5.32 ± 0.43	0.98 ± 0.01

[a] Values are the mean ± SD of three independent measurements in duplicates.

Table 2
In vitro antitumor activity of **15a**-**15n** against different cancer cell lines.

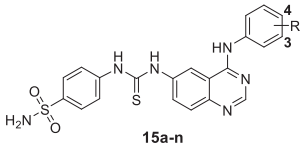

15a-n

Compounds	R	IC_{50} (μM)[a]		
		A549	A431	H1975
15a	3-Cl, 4-F	>40	37.61 ± 1.17	15.75 ± 0.11
15b	3 − *C≡CH*	>40	15.29 ± 0.21	13.42 ± 0.23
15c	3-CF_3	10.14 ± 0.24	21.68 ± 0.16	7.59 ± 0.21
15d	3-CF_3, 4-Cl	4.50 ± 0.28	18.18 ± 0.32	11.78 ± 0.13
15e	3-Br, 4-F	>40	18.21 ± 0.45	9.98 ± 0.26
15f	3-Br	25.04 ± 0.65	20.74 ± 0.73	10.96 ± 0.37
15g	4-CF_3	>40	17.96 ± 0.74	17.09 ± 0.25
15h	2-F, 3-Cl	>40	13.11 ± 0.63	25.14 ± 0.82
15i	3-F	25.88 ± 1.04	30.08 ± 1.78	9.66 ± 0.15
15j	3-Cl	>40	14.98 ± 0.34	39.79 ± 1.48
15k	3-CH_3	>40	23.79 ± 1.26	35.44 ± 0.41
15l	4-CH_3	2.84 ± 0.29	40.02 ± 2.04	39.44 ± 0.41
15 m	4-CH_2CH_3	24.64 ± 0.87	38.43 ± 1.85	38.71 ± 0.67
15n	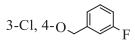	>40	29.51 ± 0.87	10.34 ± 0.17
Gefitinib		15.59 ± 1.03	8.37 ± 0.46	10.78 ± 0.45
Erlotinib		16.43 ± 0.96	11.85 ± 0.69	13.12 ± 0.97
Osimertinib		–	5.32 ± 0.43	0.98 ± 0.01

[a] Values are the mean ± SD of three independent measurements in duplicates.

Table 3
In vitro antitumor activity of **18a**-**18n** against different cancer cell lines.

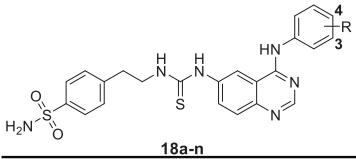

18a-n

Compounds	R	IC_{50} (μM)[a]		
		A549	A431	H1975
18a	3-Cl, 4-F	4.18 ± 0.12	16.72 ± 0.67	11.37 ± 0.16
18b	3 − *C≡CH*	3.87 ± 0.15	12.51 ± 0.16	12.67 ± 0.13
18c	3-CF_3	9.05 ± 0.31	16.76 ± 0.13	4.25 ± 0.21
18d	3-CF_3, 4-Cl	30.37 ± 1.32	21.25 ± 1.33	39.52 ± 1.22
18e	3-Br, 4-F	5.40 ± 0.54	21.08 ± 1.07	9.43 ± 0.07
18f	3-Br	9.36 ± 0.48	17.29 ± 0.75	10.76 ± 0.31
18g	4-CF_3	32.36 ± 1.35	26.71 ± 1.21	13.01 ± 0.17
18h	2-F, 3-Cl	4.53 ± 0.41	4.21 ± 0.07	13.04 ± 0.62
18i	3-F	5.51 ± 0.36	9.94 ± 0.34	35.66 ± 0.23
18j	3-Cl	2.77 ± 0.35	14.84 ± 0.95	11.01 ± 0.29
18k	3-CH_3	7.05 ± 0.58	15.99 ± 0.55	20.82 ± 0.61
18l	4-CH_3	14.66 ± 0.61	13.11 ± 0.76	10.22 ± 0.03
18 m	4-CH_2CH_3	16.62 ± 0.52	39.61 ± 2.07	9.36 ± 0.12
18n	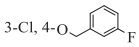	6.63 ± 0.37	5.77 ± 0.12	5.16 ± 0.05
Gefitinib		15.59 ± 1.03	8.37 ± 0.46	10.78 ± 0.45
Erlotinib		16.43 ± 0.96	11.85 ± 0.69	13.12 ± 0.97
Osimertinib		–	5.32 ± 0.43	0.98 ± 0.01

[a] Values are the mean ± SD of three independent measurements in duplicates.

to osimertinib, which may be the reason for its potent antiproliferative activity against H1975 cell line. These results suggested that substitution of morpholine for a sulfamoylphenyl group could promote the inhibitory effect on $EGFR^{T790M}$.

2.4. CA inhibition study

Since sulfonamides and their isosteres were discovered as potent carbonic anhydrase inhibitors (CAIs), some representative sulfonamide derivatives were tested to study their inhibition on cytosolic human carbonic anhydrase isoforms (CAII) and tumor associated isoforms (CAIX) using acetazolamide as positive control. The results are given in Table 4. Among the tested derivatives, **8v** exhibited the most potent inhibition on CAIX with an IC_{50} value of 115.0 nM comparable to that of acetazolamide, and showed the highest selectivity index (2.4) as well. It was noted that acetazolamide had a much stronger inhibitory effect on CAII than **8v** with a small selectivity index of 0.52, hinting its off-target disadvantage. As for other derivatives, **18c** showed stronger CA (CAII and CAIX) inhibitory activity than **15c**, which may be attributed to a longer carbon chain that enhanced the binding affinity of **18c** to CA.

2.5. Induced apoptotic cell death of 8v

According to the results of cytotoxicity assay and enzymatic inhibitory activity, apoptotic analysis of **8v** against H1975 cells were carried out by an Annexin VFITC/PI assay using gefitinib as reference. The results revealed that only a few apoptotic cells were present in the control group (6.32%) (Fig. 2). Gratifyingly, a dose-dependent increase in the percentage of apoptotic cells was observed after being treated with **8v**. The apoptosis ratio rose to 29.4% after treatment with 2 μM of **8v** for 24 h and further increased to 40.7% after treatment with 5 μM of **8v**, which was

Table 4
In vitro enzymatic inhibitory activity of representative compounds against different statues of $EGFR^{WT}$, $EGFR^{T790M}$, hCAII and hCAIX.

Compounds	IC_{50} (nM)[a]				
	$EGFR^{WT}$	$EGFR^{T790M}$	hCAII	hCAIX	SI[b]
8a	18.3 ± 5.2	61.9 ± 12.0	–	–	–
8b	13.7 ± 4.0	37.5 ± 8.2	355.8 ± 61.1	224.3 ± 45.5	1.6
8c	49.2 ± 12.3	48.5 ± 7.4	–	–	–
8 m	34.8 ± 11.5	18.0 ± 3.5	–	–	–
8v	27.0 ± 6.8	9.2 ± 2.1	278.2 ± 31.6	115.0 ± 16.8	2.4
8w	16.5 ± 3.7	22.8 ± 5.0	–	–	–
15c	51.2 ± 10.4	135.0 ± 15.2	526.2 ± 88.3	577.5 ± 94.6	0.9
18c	42.6 ± 8.5	93.4 ± 9.8	241.5 ± 43.7	312.8 ± 55.7	0.8
18n	28.4 ± 4.7	66.7 ± 5.5	–	–	–
Gefitinib	17.1 ± 4.2	378.4 ± 56.8	–	–	–
Osimertinib	58.2 ± 12.6	8.1 ± 2.2	–	–	–
Acetazolamide	–	–	45.1 ± 7.4	87.2 ± 9.6	0.5

[a] Values are the mean ± SD of three independent measurements in duplicates.
[b] Selectivity Index (SI) = hCAII IC_{50} value/hCAIX IC_{50} value.

significantly higher than that of treatment with 2 μM of gefitinib (13.22%). Overall, the results above evidently verified that compound **8v** effectively induced apoptosis in H1975 cells.

2.6. Effect on cell cycle arrest of 8v

The cell cycle is controlled by a series of checkpoints, enabling proliferation only in the presence of a stimulatory signal. The anticancer agents can arrest the cell cycle at these checkpoints [23]. In order to investigate the effect of compound **8v** on cell cycle arrest, the cycle distribution of H1975 cells treated with different concentrations of **8v** after 24 h was analyzed by flow cytometry with untreated cells as negative control and gefitinib-treated cells as positive control. The obtained data (Fig. 3) obviously indicated that compound **8v** arrested the cell cycle at the G2/M phase in a dose-dependent manner (47.44% for 2 μM and 54.85% for 5 μM), when compared to the untreated control group (14.74%). Also, gefitinib arrested the cell cycle at the G2/M phase by 33.72% at 2 μM. Cell population at the G2/M increased in comparison to control cell. These results revealed that in H1975 cells, compound **8v** evidently arrested the G2/M phase of the cell cycle in a dose-dependent manner.

2.7. Inhibition of migration

To study the effect of compound **8v** on tumor cell migration, we performed wound healing assays in H1975 cell line, in which **8v** at 0.5 and 1.0 μM was used to reduce cell killing. As shown in Fig. 4, the migration rate decreased significantly with the increase of the concentration of **8v**. After treatment with 1.0 μM of **8v**, the migration rate decreased from 51.2% to 17.9%. The results indicated that compound **8v** effectively inhibited the migration in H1975 cells.

2.8. Western blot analysis of 8v

The selective inhibition of the representative compound **8v** for the phosphorylation of EGFR and the downstream signaling transduction (AKT and ERK) was studied by the Western blot assay. As showed in Fig. 5, the results clearly showed that after **8v** treatment, p-EGFR, p-AKT and p-ERK expression levels were decreased obviously in a dose dependent manner. Interestingly, compound **8v** inhibited the phosphorylation of EGFR and downstream signaling transduction more potently than gefitinib did at 2 μM. These findings indicated that compound **8v** could specifically target EGFR and inhibit its related downstream phosphorylated protein expression.

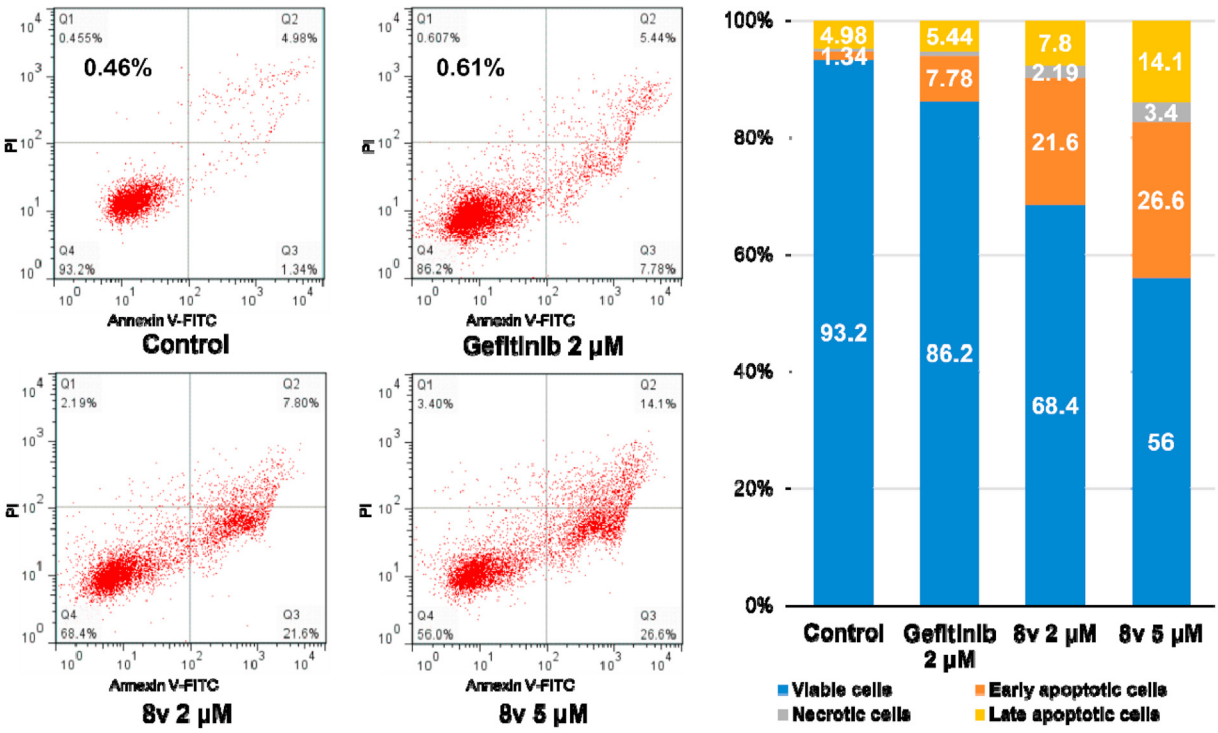

Fig. 2. Induction of apoptosis at 24 h by gefitinib and **8v** in H1975 cells. The cells were harvested and labeled with annexin-V-FITC and PI, and analyzed by flow cytometry. Data are expressed as the mean ± SEM for three independent experiments.

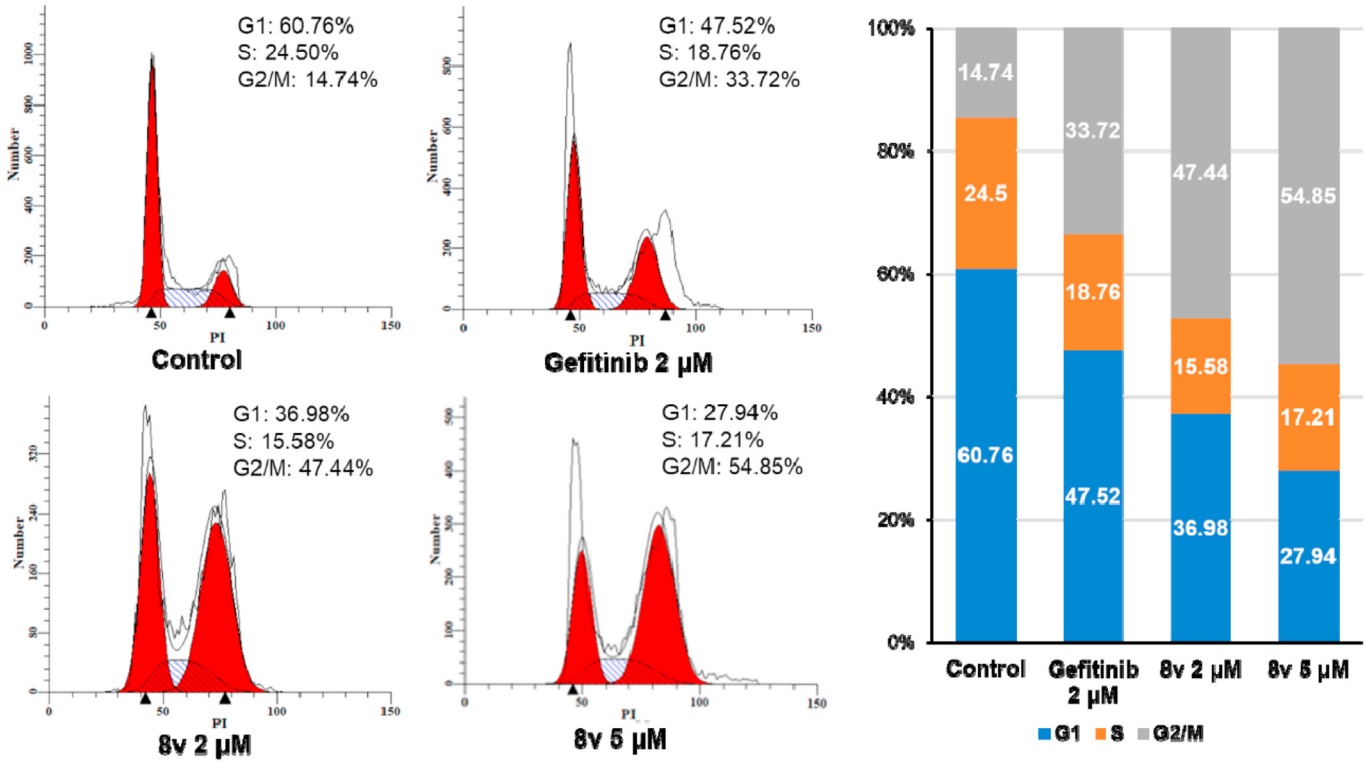

Fig. 3. Effects of gefitinib and **8v** on cell cycle arrest in H1975 cells. Cells were treated with 2 and 5 μM of **8v** for 24 h. Then the cells were fixed and stained with PI to analyze DNA content by flow cytometry.

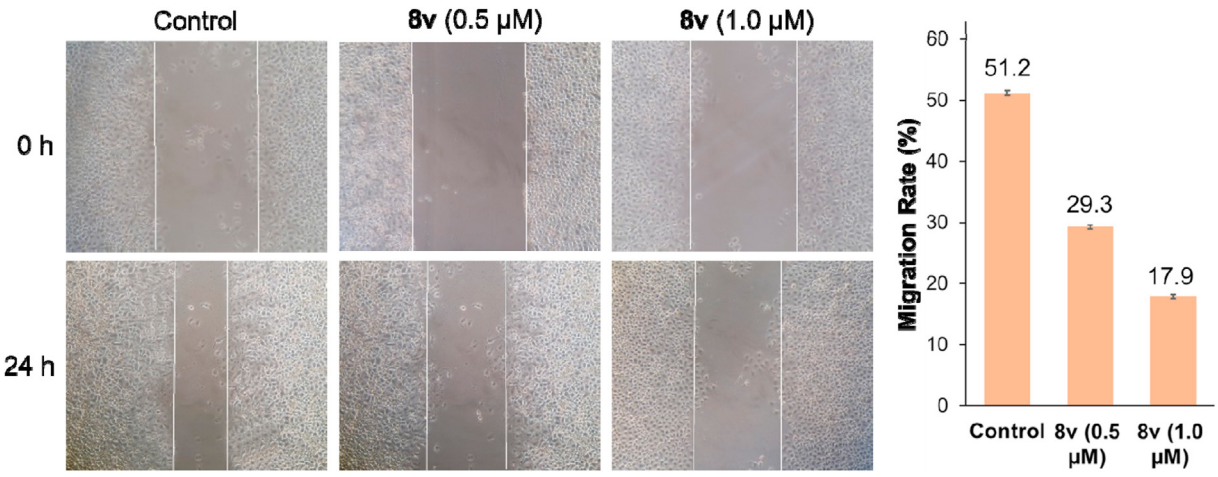

Fig. 4. Cell migration inhibition and migration rates of H1975 cells after treated with 0.5 and 1.0 μM of **8v,** respectively, for 24 h.

2.9. Cytotoxic activity and Western blot analysis of 8v under hypoxia

In order to ascertain the anti-proliferative potential of compound (**8v**) under hypoxic condition, A549 and H1975 cancer cells were treated with **8v** at the indicated concentrations for 72 h of incubation. The hypoxic condition was achieved by incubating the cells under a hypoxic atmosphere (1% O_2, 5% CO_2, and N_2 94%). As shown in Table 5, **8v** caused about 3 times increase in anticancer activity towards A549 under the hypoxic condition compared with that under the normoxic condition, and the anticancer activity of **8v** towards H1975 cells was about 2 times better than that of under normoxic condition. Interestingly, osimertinib presented converse results against H1975 cells under hypoxic and normoxic conditions. These findings motivated us to further explore the antiproliferative mechanism of compound **8v** under hypoxia.

To further evaluate the effect of **8v** on the expression of CAIX, we performed Western blot analysis of the compound towards H1975 cells under hypoxic condition using acetazolamide as positive control. As shown in Fig. 6, acetazolamide successfully inhibited the expression of CAIX at 2 μM under hypoxic condition. As expected, **8v** also significantly down-regulated the expression level of CAIX protein in a dose dependent manner. Since CAIX expression on the cell surface is regulated by HIF-1α, the effect of **8v** on the expression of HIF-1α was also determined. Interestingly, like CAIX, **8v** obviously down-regulated the expression level of HIF-1α protein

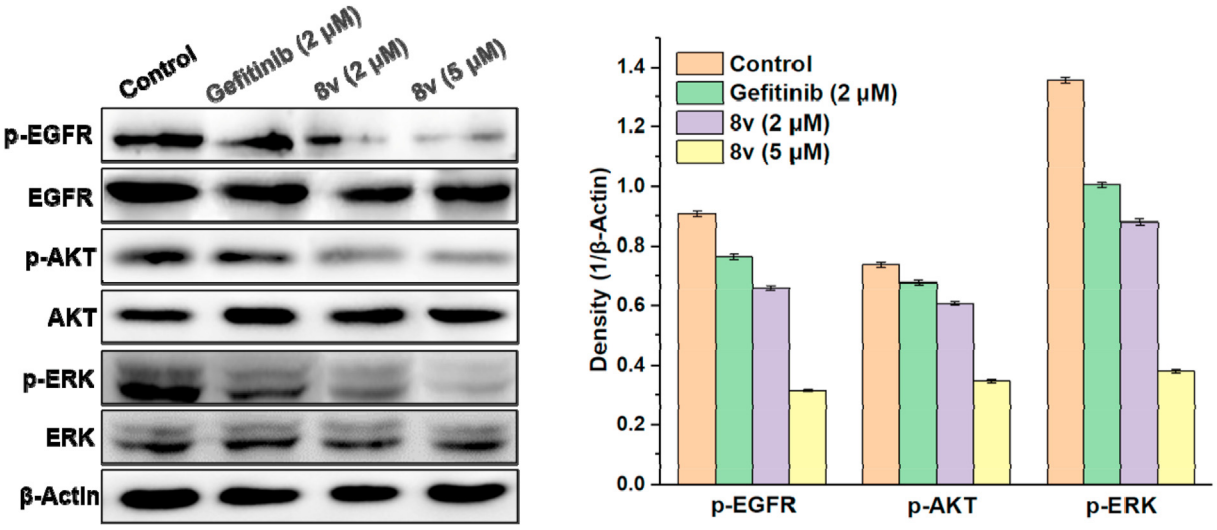

Fig. 5. Western blot and statistical analysis of the expression level of EGFR, p-EGFR, AKT, p-AKT, ERK and p-ERK in H1975 cells induced by gefitinib and **8v** based on three independent experiments.

Table 5
Cytotoxic effects of **8v** against A549 and H1975 cells under hypoxic or normoxic conditions.

Compounds	Hypoxia IC_{50} (μM)[a]		Normoxia IC_{50} (μM)[a]	
	A549	H1975	A549	H1975
8v	2.21 ± 0.09	1.05 ± 0.08	6.54 ± 0.59	1.94 ± 0.14
Osimertinib	–	2.08 ± 0.03	–	0.98 ± 0.01

[a] Values are the mean ± SD of three independent measurements in duplicates.

in a dose dependent manner. These results indicated that introduction of sulfonamides moieties gave **8v** the ability to inhibit the expression of CAIX and upstream HIF-1α protein.

2.10. Molecular docking study of 8v

In order to better illustrate the structural basis of our EGFR and CAIX dual inhibitors, molecular docking was performed on the basis of co-crystallization of $EGFR^{WT}$, $EGFR^{T790M}$ and CAIX.

According to the *in vitro* antiproliferation activity of the target compounds, compound **8v** was selected to conduct molecular docking study by the PYMOL software with $EGFR^{WT}$ protein (PDB code:2ITY) [24] and $EGFR^{T790M}$ mutant protein (PDB code:2JIU) [25]. In the $EGFR^{WT}$ binding model (Fig. 7), the nitrogen atoms in quinazoline of **8v** can bind to Met793 residue by hydrogen bonds, which is consistent with the binding site of gefitinib in EGFR domain. Besides, the sulfa warhead of **8v** forms hydrogen bonding with the residue Lys-745 in $EGFR^{WT}$, due to the U-shaped structure. In $EGFR^{T790M}$, **8v** maintains the same binding pose as in $EGFR^{WT}$ (Fig. 7). As expected, the quinazoline core forms the classical hydrogen bond interactions with Met793. Interestingly, the sulfa warhead of **8v** forms more hydrogen bonds with Arg-841, Asp-855 and Lys-745 in $EGFR^{T790M}$ than those in $EGFR^{WT}$, which lead to the binding force of **8v** and kinase $EGFR^{T790M}$ more closely and firmly. This may be the reason that **8v** had strong inhibitory activity and selectivity to $EGFR^{T790M}$ kinase.

For the purpose of exploring the binding interaction of compound **8v** within CAIX active site, co-crystallization of CAIX protein with acetazolamide (PDB code:3IAI) was selected. As shown in Fig. 8, major interactions of **8v** with the enzyme active site are mediated through the deeply buried sulfonamide group, which make residues locate at the bottom of the active site cavity (Thr199 and Thr200), similar to the binding site of acetazolamide in CAIX

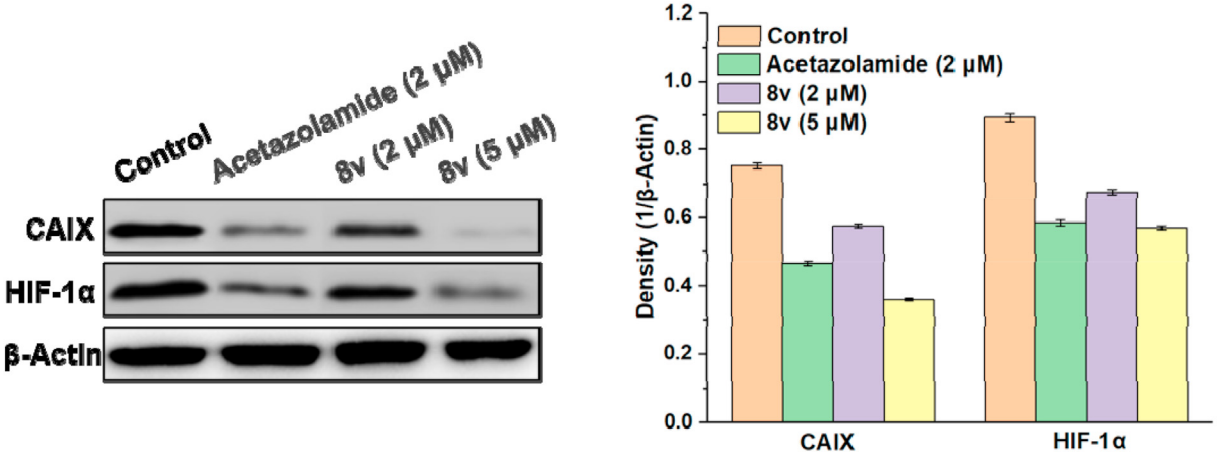

Fig. 6. Western blot and statistical analysis of the expression level of CAIX and HIF-1α in H1975 cells under hypoxic condition. Data represent three individual experiments.

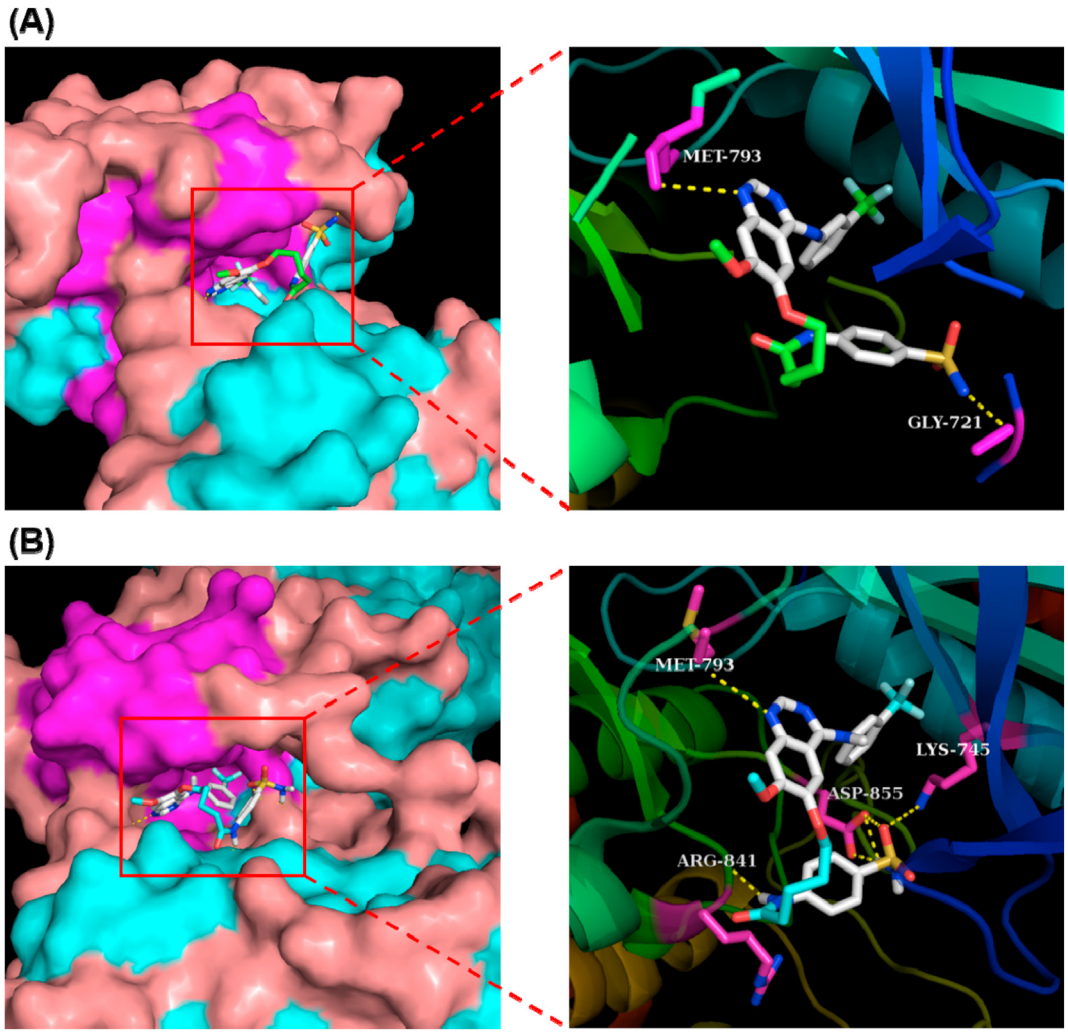

Fig. 7. 3D model of **8v** bound to $EGFR^{WT}$ and $EGFR^{T790M}$. (A) 3D model of **8v** bound to $EGFR^{WT}$ (PDB code:2ITY). (B) 3D model of **8v** bound to $EGFR^{T790M}$ (PDB code:2JIU).

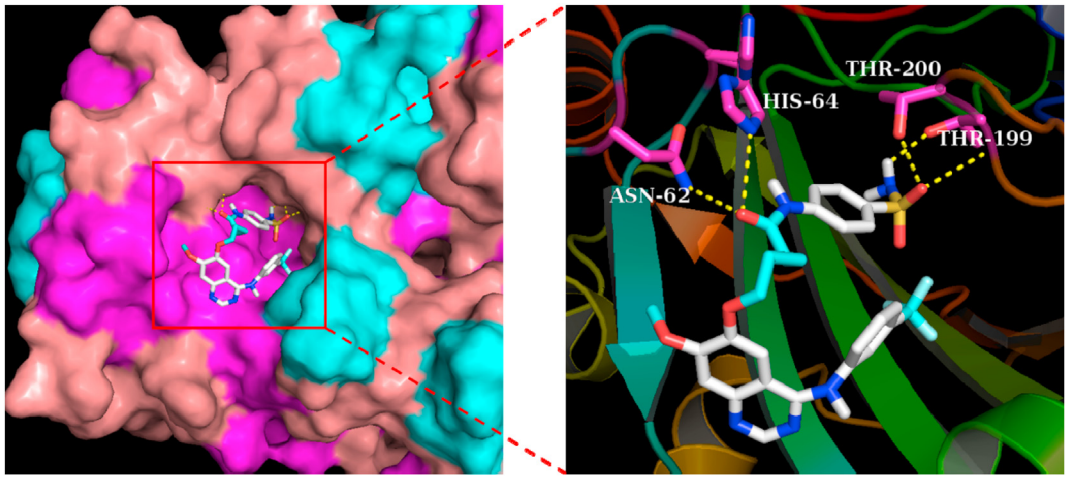

Fig. 8. 3D model of **8v** bound to CAIX (PDB code:3IAI).

domain. In addition, the oxygen atom of the amide bond forms two additional hydrogen bonds with residue Asn62 and His64, which might enhance the binding affinity of **8v** to CAIX protein.

These docking results suggest that compound **8v** could successfully bind to $EGFR^{WT}$, $EGFR^{T790M}$ and CAIX protein. Besides, the binding of **8v** to $EGFR^{T790M}$ is more favorable than its binding to

$EGFR^{WT}$, which is in good agreement with the experimental results. Upon the molecular docking diagram, we can conclude that the design idea of EGFR and CAIX dual inhibitors are rational.

3. Conclusions

Three different series of quinazoline derivatives bearing benzene-sulfonamide moiety were prepared and biologically evaluated as dual EGFR/CAIX inhibitors. All compounds were examined for their anti-proliferative activity against human epidermoid carcinoma (A431) and non-small cell lung cancer (A549 and H1975) cell lines. Among the synthesized compounds, **8v** exhibited comparable activity to osimertinib against mutant-type non-small cell lung cancer cell line H1975. Furthermore, **8v** displayed stronger anti-proliferative activity than osimertinib against H1975 cells under hypoxic condition. The SAR studies revealed that introduction of a trifluoromethyl group at 3-positon of the aryl group and the increase in the length of the carbon chain between two pharmacophores were beneficial to promote the antitumor activity of the resulting compound. Several representative compounds exhibited good to excellent inhibitory activities against $EGFR^{WT}$ and $EGFR^{T790M}$ enzymes. It is worth noting that **8v** showed excellent inhibitory effect on $EGFR^{T790M}$, which was 41 times more effective than gefitinib and almost equal to osimertinib. Mechanism study indicated that **8v** exhibited remarkable CAIX inhibitory effect comparable to acetazolamide, and it could significantly inhibit the expression of p-EGFR and its downstream p-AKT and p-ERK in H1975 cells. More importantly, **8v** could also successfully inhibit the expression of CAIX and its upstream HIF-1α in H1975 cells under hypoxic condition. Molecular docking studies illustrated the binding pattern of **8v** with $EGFR^{WT}$, $EGFR^{T790M}$ and CAIX proteins, which validated the rational of our design for EGFR and CAIX dual inhibitors. Therefore, our research offers a promising way for development of potent multi-target anticancer agents.

4. Experimental

4.1. Materials and instruments

All chemical reagents and solvents used in experiments were purchased from commercial suppliers and used without further purification. Thin-layer chromatography (TLC) used to monitor progress of the reaction and column chromatography was performed using silica gel (200–300 mesh). ^1H and ^{13}C NMR spectra were recorded with a Bruker spectrometer at 600 and 150 MHz, respectively. Mass spectra were measured by an Agilent 6224 ESI/TOF MS instrument. The purity of final compounds was analyzed by RP-HPLC (Waters e2695) using gradient elution with an eluent of methanol/water (20:80 to 100:0, V/V) (0.1% trifluoroacetic acid in water). All of the compounds submitted for biological studies were at least 95%. Besides, all cells used in this article were obtained from KeyGEN BioTECH Corp. Recombinant human carbonic anhydrase II and IX were purchased from Sino Biological Inc. Antibodies directed against p-EGFR, EGFR, p-MEK, MEK, p-ERK, ERK, CAIX and HIF-1α were purchased from Abcam.

4.2. General methods for preparation of compounds

4.2.1. Synthesis of 5-bromo-N-(4-sulfamoylphenyl)pentanamide (7)

To a solution of compound 5 (344 mg, 2.0 mmol) in dry DMF (10 mL), pyridine (316 mg, 4.0 mmol) was added. After stirred at 0 °C for 5 min, compound **6** (598 mg, 3.0 mmol) was added. The reaction was stirred at room temperature overnight and monitored by TLC. After completion of reaction, the reaction mixture was poured into water (250 mL) with stirring to give a white precipitate. The precipitate was purified on silica gel column eluted with DCM/MeOH (20:1 v/v) to give compound **7** (412 mg, yield 58.6%) as a white solid. ^1H NMR (600 MHz, DMSO-d_6) δ 10.25 (s, 1H), 7.74 (s, 4H), 7.24 (s, 2H), 3.56 (t, J = 6.6 Hz, 2H), 2.39 (t, J = 7.3 Hz, 2H), 1.87–1.82 (m, 2H), 1.74–1.69 (m, 2H).

4.2.2. Synthesis of 6-hydroxyl-7-methoxy-4-arylaminoquinazolines (4a-w)

Compounds **4a-w** were prepared according to reported procedures [20].

4.2.3. Synthesis of 5-((7-methoxy-4-((substituted phenyl)amino) quinazolin-6-yl)oxy)- N-(4-sulfamoylphenyl)pentanamides (8a-w)

A mixture of intermediates **4a-w** (0.25 mmol) and K_2CO_3 (69 mg, 0.5 mmol) in anhydrous DMF (5 mL) was stirred at room temperature. Then KI (9 mg, 0.05 mmol) and compound **7** (100 mg, 0.3 mmol) were added to the mixture and stirred at 60 °C overnight. After completion of reaction, the mixture was treated with water and extracted with dichloromethane. The combined organic layers were washed with water and brine, dried over Na_2SO_4, and concentrated. The residue was purified on silica gel column eluted with DCM/MeOH (20:1 v/v) to give the desired products **8a-w**.

4.2.3.1. 5-((4-((3-chloro-4-fluorophenyl)amino)-7-methoxy quinazolin-6-yl)oxy)- *N*-(4-sulfamoylphenyl)pentanamide (**8a**). Yellow solid (yield: 61.5%). ^1H NMR (600 MHz, DMSO-d_6) δ 10.29 (s, 1H), 9.52 (s, 1H), 8.50 (s, 1H), 8.12 (d, J = 4.8 Hz, 1H), 7.80 (s, 2H), 7.76 (s, 4H), 7.44 (t, J = 9.0 Hz, 1H), 7.26 (s, 2H), 7.19 (s, 1H), 4.23–4.11 (m, 2H), 3.93 (s, 3H), 2.50–2.42 (m, 2H), 1.95–1.77 (m, 4H). ^{13}C NMR (150 MHz, DMSO-d_6) δ 171.68, 156.01, 154.51, 153.17 (d, J = 241.5 Hz), 152.63, 148.36, 146.96, 142.20, 138.12, 136.82 (d, J = 2.9 Hz), 126.71, 123.51, 122.34 (d, J = 6.9 Hz), 118.80 (d, J = 18.3 Hz), 118.56, 116.53 (d, J = 21.5 Hz), 108.78, 107.29, 102.43, 68.52, 55.89, 36.05, 28.20, 21.76. HRMS (*m/z*) (ESI): calcd for $C_{26}H_{26}ClFN_5O_5S$ $[M+H]^+$: 574.1322; found: 574.1321.

4.2.3.2. 5-((4-((4-chloro-3-(trifluoromethyl)phenyl)amino)-7-methoxyquinazolin -6-yl)oxy)-*N*-(4-sulfamoylphenyl)pentanamide (**8b**). Yellow solid (yield: 68.0%). ^1H NMR (600 MHz, DMSO-d_6) δ 10.31 (s, 1H), 9.72 (s, 1H), 8.54 (s, 1H), 8.38 (s, 1H), 8.28 (d, J = 8.0 Hz, 1H), 7.82 (s, 1H), 7.75–7.71 (m, 5H), 7.26–7.21 (m, 3H), 4.23–4.18 (m, 2H), 3.94 (s, 3H), 2.50–2.47 (m, 2H), 1.94–1.89 (m, 2H), 1.84–1.77 (m, 2H). ^{13}C NMR (150 MHz, DMSO-d_6) δ 171.71, 155.81, 154.69, 152.44, 148.53, 147.16, 142.22, 139.28, 138.13, 131.72, 126.73, 126.54, 126.34, 123.42, 122.96 (d, J = 270.0 Hz), 120.21 (d, J = 6.0 Hz), 118.57, 108.99, 107.32, 102.40, 68.58, 55.96, 36.06, 28.22, 21.79. HRMS (*m/z*) (ESI): calcd for $C_{27}H_{26}ClF_3N_5O_5S$ $[M+H]^+$: 624.1290; found: 624.1281.

4.2.3.3. 5-((4-((3-ethynylphenyl)amino)-7-methoxyquinazolin-6-yl)oxy)-*N*-(4- sulfamoylphenyl)pentanamide (**8c**). Yellow solid (yield: 67.4%). ^1H NMR (600 MHz, DMSO-d_6) δ 10.28 (s, 1H), 9.48 (s, 1H), 8.50 (s, 1H), 7.99 (s, 1H), 7.90 (dd, J = 8.3, 1.2 Hz, 1H), 7.84 (s, 1H), 7.77–7.74 (m, 4H), 7.40 (t, J = 7.9 Hz, 1H), 7.25 (s, 2H), 7.21 (d, J = 7.6 Hz, 1H), 7.20 (s, 1H), 4.20 (s, 1H), 4.19 (t, J = 6.3 Hz, 2H), 3.93 (s, 3H), 2.48 (t, J = 7.2 Hz, 2H), 1.92–1.88 (m, 2H), 1.86–1.81 (m, 2H). ^{13}C NMR (150 MHz, DMSO-d_6) δ 171.68, 156.12, 154.47, 152.72, 148.33, 147.00, 142.20, 139.83, 138.12, 128.92, 126.71, 126.38, 124.84, 122.66, 121.76, 118.56, 108.92, 107.30, 102.53, 83.53, 80.59, 68.52, 55.89, 36.04, 28.19, 21.76. HRMS (*m/z*) (ESI): calcd for $C_{28}H_{28}N_5O_5S$ $[M+H]^+$: 546.1806; found: 546.1824.

4.2.3.4. 5-((4-((3-chloro-4-fluorophenyl)amino)-7-methoxy quinazolin-6-yl)oxy) -*N*-(4-sulfamoylphenyl)pentanamide (**8d**). Yellow solid (yield: 65.3%). ^1H NMR (600 MHz, DMSO-d_6) δ 10.29 (s, 1H), 9.51 (s, 1H), 8.52 (s, 1H), 8.15 (s, 1H), 7.89 (d, J = 8.1 Hz, 1H), 7.84 (s, 1H), 7.77–7.74 (m, 4H), 7.35 (t, J = 8.0 Hz, 1H), 7.28 (d, J = 8.7 Hz, 1H), 7.26 (s, 2H), 7.20 (s, 1H), 4.19 (t, J = 6.1 Hz, 2H), 3.93 (s, 3H), 2.48 (t, J = 7.2 Hz, 2H), 1.92–1.87 (m, 2H), 1.85–1.81 (m, 2H). ^{13}C NMR

(150 MHz, DMSO-d_6) δ 171.69, 155.99, 154.53, 152.64, 148.39, 147.04, 142.21, 141.31, 138.12, 130.39, 126.72, 125.63, 124.07, 121.21, 120.64, 118.56, 108.95, 107.30, 102.48, 68.54, 55.91, 36.04, 28.20, 21.77. HRMS (*m/z*) (ESI): calcd for $C_{26}H_{27}BrN_5O_5S$ $[M+H]^+$: 600.0911; found: 600.0848.

4.2.3.5. 5-((4-((3-chlorophenyl)amino)-7-methoxyquinazolin-6-yl)oxy)-*N*-(4- sulfamoylphenyl)pentanamide (**8e**). Yellow solid (yield: 64.5%). ^{1}H NMR (600 MHz, DMSO-d_6) δ 10.30 (s, 1H), 9.54 (s, 1H), 8.53 (s, 1H), 8.04 (s, 1H), 7.85 (s, 1H), 7.82 (d, J = 8.3 Hz, 1H), 2.78−7.74 (m, 4H), 7.41 (t, J = 8.1 Hz, 1H), 7.26 (s, 2H), 7.21 (s, 1H), 7.15 (d, J = 7.1 Hz, 1H), 4.19 (t, J = 6.0 Hz, 2H), 3.94 (s, 3H), 2.50−2.45 (m, 2H), 1.91−1.82 (m, 4H). ^{13}C NMR (150 MHz, DMSO-d_6) δ 171.69, 156.02, 154.54, 152.63, 148.39, 147.01, 142.21, 141.16, 138.12, 132.75, 130.07, 126.71, 122.75, 121.29, 120.24, 118.56, 108.95, 107.28, 102.51, 68.55, 55.91, 36.04, 28.19, 21.77. HRMS (*m/z*) (ESI): calcd for $C_{26}H_{27}ClN_5O_5S$ $[M+H]^+$: 556.1416; found: 556.1399.

4.2.3.6. 5-((4-((3-fluorophenyl)amino)-7-methoxyquinazolin-6-yl)oxy)-*N*-(4- sulfamoylphenyl)pentanamide (**8f**). Yellow solid (yield: 70.5%). ^{1}H NMR (600 MHz, DMSO-d_6) δ 10.31 (s, 1H), 9.57 (s, 1H), 8.52 (s, 1H), 7.90 (d, J = 11.9 Hz, 1H), 7.86 (s, 1H), 7.78−7.73 (m, 4H), 7.62 (d, J = 7.9 Hz, 1H), 7.43−7.39 (m, 1H), 7.26 (s, 2H), 7.21 (s, 1H), 6.93−6.90 (m, 1H), 4.20 (t, J = 6.0 Hz, 2H), 3.94 (s, 3H), 2.50−2.47 (m, 2H), 1.91−1.81 (m, 4H). ^{13}C NMR (150 MHz, DMSO-d_6) δ 171.70, 162.07 (d, J = 238.5 Hz), 156.07, 154.53, 152.64, 148.38, 147.05, 142.22, 141.46 (d, J = 10.5 Hz), 138.12, 129.91 (d, J = 9.0 Hz), 126.72, 118.57, 117.53 (d, J = 3.0 Hz), 109.50 (d, J = 21.0 Hz), 108.99, 108.64 (d, J = 25.5 Hz), 107.31, 102.57, 68.57, 55.91, 36.04, 28.20, 21.78. HRMS (*m/z*) (ESI): calcd for $C_{26}H_{27}FN_5O_5S$ $[M+H]^+$: 540.1711; found: 540.1677.

4.2.3.7. 5-((4-((4-fluorophenyl)amino)-7-methoxyquinazolin-6-yl)oxy)-*N*-(4- sulfamoylphenyl)pentanamide (**8g**). Yellow solid (yield: 65.5%). ^{1}H NMR (600 MHz, DMSO-d_6) δ 10.30 (s, 1H), 9.52 (s, 1H), 8.43 (s, 1H), 7.84 (s, 1H), 7.79−7.74 (m, 6H), 7.26 (s, 2H), 7.23 (t, J = 8.8 Hz, 2H), 7.18 (s, 1H), 4.18 (t, J = 6.1 Hz, 2H), 3.93 (s, 3H), 2.50−2.46 (m, 2H), 1.91−1.81 (m, 4H). ^{13}C NMR (150 MHz, DMSO-d_6) δ 171.70, 159.18, 157.59, 156.45, 153.60 (d, J = 237.0 Hz), 148.24, 146.71, 142.22, 138.12, 135.67, 126.72, 124.53 (d, J = 7.5 Hz), 118.57, 115.05 (d, J = 22.5 Hz), 108.74, 107.17, 102.66, 68.52, 55.87, 36.04, 28.19, 21.77. HRMS (*m/z*) (ESI): calcd for $C_{26}H_{27}FN_5O_5S$ $[M+H]^+$: 540.1711; found: 540.1657.

4.2.3.8. 5-((4-((4-chlorophenyl)amino)-7-methoxyquinazolin-6-yl)oxy)-*N*-(4- sulfamoylphenyl)pentanamide (**8h**). Yellow solid (yield: 73.2%). ^{1}H NMR (600 MHz, DMSO-d_6) δ 10.29 (s, 1H), 9.54 (s, 1H), 8.48 (s, 1H), 7.87−7.84 (m, 3H), 7.77−7.74 (m, 4H), 7.45−7.43 (m, 2H), 7.25 (s, 2H), 7.19 (s, 1H), 4.18 (t, J = 6.2 Hz, 2H), 3.93 (s, 3H), 2.48 (t, J = 7.4 Hz, 2H), 1.92−1.80 (m, 4H). ^{13}C NMR (150 MHz, DMSO-d_6) δ 171.68, 156.15, 154.48, 152.67, 148.32, 146.86, 142.20, 138.50, 138.12, 128.33, 126.91, 126.71, 123.76, 118.56, 108.90, 107.22, 102.60, 68.53, 55.90, 36.04, 28.19, 21.76. HRMS (*m/z*) (ESI): calcd for $C_{26}H_{27}ClN_5O_5S$ $[M+H]^+$: 556.1416; found: 556.1381.

4.2.3.9. 5-((4-((4-bromophenyl)amino)-7-methoxyquinazolin-6-yl)oxy)-*N*-(4- sulfamoylphenyl)pentanamide (**8i**). Yellow solid (yield: 68.3%). ^{1}H NMR (600 MHz, DMSO-d_6) δ 10.29 (s, 1H), 9.53 (s, 1H), 8.48 (s, 1H), 7.85 (s, 1H), 7.82 (d, J = 8.7 Hz, 2H), 7.77−7.74 (m, 4H), 7.56 (d, J = 8.7 Hz, 2H), 7.25 (s, 2H), 7.19 (s, 1H), 4.18 (t, J = 6.0 Hz, 2H), 3.93 (s, 3H), 2.50−2.46 (m, 2H), 1.90−1.80 (m, 4H). ^{13}C NMR (150 MHz, DMSO-d_6) δ 171.67, 156.09, 154.48, 152.65, 148.32, 146.88, 142.20, 138.95, 138.11, 131.22, 126.70, 124.07, 118.55, 114.92, 108.92, 107.22, 102.60, 68.53, 55.89, 36.03, 28.18, 21.75. HRMS (*m/z*) (ESI): calcd for $C_{26}H_{27}BrN_5O_5S$ $[M+H]^+$: 600.0911; found: 600.0835.

4.2.3.10. 5-((7-methoxy-4-((4-methoxyphenyl)amino)quinazolin-6-yl)oxy)-*N*-(4- sulfamoylphenyl)pentanamide (**8j**). Yellow solid (yield: 62.7%). ^{1}H NMR (600 MHz, DMSO-d_6) δ 10.30 (s, 1H), 9.44 (s, 1H), 8.39 (s, 1H), 7.85 (s, 1H), 7.77−7.74 (m, 4H), 7.62 (d, J = 9.0 Hz, 2H), 7.25 (s, 2H), 7.16 (s, 1H), 6.97 (d, J = 9.0 Hz, 2H), 4.17 (t, J = 6.2 Hz, 2H), 3.92 (s, 3H), 3.77 (s, 3H), 2.50−2.45 (m, 2H), 1.90−1.80 (m, 4H). ^{13}C NMR (150 MHz, DMSO-d_6) δ 171.69, 156.70, 155.78, 154.25, 152.92, 148.10, 146.31, 142.21, 138.11, 132.11, 126.70, 124.62, 118.56, 113.67, 108.66, 106.98, 102.77, 68.49, 55.83, 55.24, 36.03, 28.17, 21.76. HRMS (*m/z*) (ESI): calcd for $C_{27}H_{30}N_5O_6S$ $[M+H]^+$: 552.1911; found: 552.1881.

4.2.3.11. 5-((4-((3,4-dimethoxyphenyl)amino)-7-methoxyquinazolin-6-yl)oxy)- *N*-(4-sulfamoylphenyl)pentanamide (**8k**). Yellow solid (yield: 63.0%). ^{1}H NMR (600 MHz, DMSO-d_6) δ 10.29 (s, 1H), 9.39 (s, 1H), 8.41 (s, 1H), 7.84 (s, 1H), 7.78−7.73 (m, 4H), 7.36 (d, J = 2.3 Hz, 1H), 7.30−7.28 (m, 1H), 7.24 (s, 2H), 7.16 (s, 1H), 6.98 (d, J = 8.7 Hz, 1H), 4.18 (t, J = 5.8 Hz, 2H), 3.92 (s, 3H), 3.78 (s, 3H), 3.77 (s, 3H), 2.47 (t, J = 6.7 Hz, 2H), 1.91−1.83 (m, 4H). ^{13}C NMR (150 MHz, DMSO-d_6) δ 171.66, 156.64, 154.24, 152.93, 148.44, 148.09, 146.48, 145.40, 142.18, 138.11, 132.58, 126.67, 118.54, 115.21, 111.80, 108.73, 108.17, 107.09, 102.78, 68.52, 55.81, 55.77, 55.61, 36.02, 28.17, 21.75. HRMS (*m/z*) (ESI): calcd for $C_{28}H_{32}N_5O_7S$ $[M+H]^+$: 582.2017; found: 582.1990.

4.2.3.12. 5-((4-((3-bromo-4-fluorophenyl)amino)-7-methoxyquinazolin-6-yl)oxy) -*N*-(4-sulfamoylphenyl)pentanamide (**8l**). Yellow solid (yield: 64.5%). ^{1}H NMR (600 MHz, DMSO-d_6) δ 10.28 (s, 1H), 9.53 (s, 1H), 8.50 (s, 1H), 8.21 (dd, J = 6.4, 2.6 Hz, 1H), 7.89−7.85 (m, 1H), 7.82 (s, 1H), 7.75 (s, 4H), 7.41 (t, J = 8.8 Hz, 1H), 7.24 (s, 2H), 7.20 (s, 1H), 4.18 (t, J = 5.9 Hz, 2H), 3.93 (s, 3H), 2.50−2.47 (m, 2H), 1.93−1.77 (m, 4H). ^{13}C NMR (150 MHz, DMSO-d_6) δ 171.63, 155.42, 155.26 (d, J = 224.4 Hz), 153.02, 152.59, 148.34, 146.89, 142.17, 138.10, 137.03 (d, J = 4.1 Hz), 126.66, 126.21, 123.03 (d, J = 6.8 Hz), 118.53, 116.32 (d, J = 22.8 Hz), 108.75, 107.28, 107.16 (d, J = 27.6 Hz), 102.48, 68.52, 55.87, 36.01, 28.16, 21.72. HRMS (*m/z*) (ESI): calcd for $C_{26}H_{26}BrFN_5O_5S$ $[M+H]^+$: 618.0817; found: 618.0824.

4.2.3.13. 5-((4-((3-chloro-2-fluorophenyl)amino)-7-methoxyquinazolin-6-yl)oxy) -*N*-(4-sulfamoylphenyl)pentanamide (**8m**). Yellow solid (yield: 67.8%). ^{1}H NMR (600 MHz, DMSO-d_6) δ 10.30 (s, 1H), 9.65 (s, 1H), 8.38 (s, 1H), 7.82 (s, 1H), 7.77−7.74 (m, 4H), 7.52 (t, J = 7.1 Hz, 1H), 7.48 (t, J = 7.0 Hz, 1H), 7.28 (t, J = 8.1 Hz, 1H), 7.25 (s, 2H), 7.21 (s, 1H), 4.17 (t, J = 6.2 Hz, 2H), 3.94 (s, 3H), 2.48 (t, J = 7.7 Hz, 2H), 1.91−1.87 (m, 2H), 1.84−1.80 (m, 2H). ^{13}C NMR (150 MHz, DMSO-d_6) δ 171.68, 156.90, 153.77 (d, J = 240.0 Hz), 153.33, 151.68, 148.34, 146.93, 142.21, 138.11, 128.40 (d, J = 11.9 Hz), 127.18, 126.98, 126.71, 124.94 (d, J = 4.4 Hz), 120.18 (d, J = 16.5 Hz), 118.56, 108.66, 107.13, 102.56, 68.41, 55.91, 36.02, 28.14, 21.73. HRMS (*m/z*) (ESI): calcd for $C_{26}H_{26}ClFN_5O_5S$ $[M+H]^+$: 574.1322; found: 574.1343.

4.2.3.14. 5-((7-methoxy-4-((4-(trifluoromethoxy)phenyl) amino)quinazolin-6- yl)oxy)-*N*-(4-sulfamoylphenyl)pentanamide (**8n**). Yellow solid (yield: 69.3%). ^{1}H NMR (600 MHz, DMSO-d_6) δ 10.28 (s, 1H), 9.59 (s, 1H), 8.48 (s, 1H), 7.92 (d, J = 9.0 Hz, 2H), 7.85 (s, 1H), 7.78−7.73 (m, 4H), 7.39 (d, J = 8.7 Hz, 2H), 7.24 (s, 2H), 7.20 (s, 1H), 4.19 (t, J = 5.7 Hz, 2H), 3.94 (s, 3H), 2.47 (d, J = 6.8 Hz, 2H), 1.91−1.83 (m, 4H). ^{13}C NMR (150 MHz, DMSO-d_6) δ 171.64, 156.17, 154.51, 152.65, 148.32, 146.94, 143.65, 142.17, 138.74, 138.11, 126.67, 123.55, 121.22, 120.21 (d, J = 254.0 Hz), 118.54, 108.86, 107.24, 102.64, 68.54, 55.87, 36.01, 28.16, 21.73. HRMS (*m/z*) (ESI): calcd for $C_{27}H_{27}F_3N_5O_6S$ $[M+H]^+$: 606.1629; found: 606.1607.

4.2.3.15. 5-((7-methoxy-4-(m-tolylamino)quinazolin-6-yl)oxy)-*N*-(4- sulfamoylphenyl)pentanamide (**8o**). Yellow solid (yield: 67.7%). ^{1}H NMR (600 MHz, DMSO-d_6) δ 10.29 (s, 1H), 9.42 (s, 1H), 8.45 (s, 1H), 7.87 (s, 1H), 7.78−7.73 (m, 4H), 7.63 (d, J = 8.2 Hz, 1H), 7.58 (s, 1H), 7.29−7.24 (m, 3H), 7.18 (s, 1H), 6.94 (d, J = 7.5 Hz, 1H), 4.19 (t, J = 5.8 Hz, 2H), 3.93 (s, 3H), 2.50−2.45 (m, 2H), 2.34 (s, 3H), 1.91−1.83 (m, 4H). ^{13}C NMR (150 MHz, DMSO-d_6) δ 171.64, 156.42, 154.35, 152.78, 148.19, 146.55, 142.17, 139.29, 138.10, 137.56, 128.25, 126.66, 124.18, 122.93, 119.69, 118.53, 108.83, 107.06, 102.72, 68.50,

55.83, 36.01, 28.15, 21.73, 21.16. HRMS (*m/z*) (ESI): calcd for $C_{27}H_{30}N_5O_5S$ $[M+H]^+$: 536.1962; found: 536.1930.

4.2.3.16. 5-((7-methoxy-4-((3,4,5-trifluorophenyl)amino)quinazolin-6-yl)oxy)- *N*-(4-sulfamoylphenyl)pentanamide (**8p**). Yellow solid (yield: 67.0%). ^{1}H NMR (600 MHz, DMSO-d_6) δ 10.28 (s, 1H), 9.56 (s, 1H), 8.55 (s, 1H), 7.90–7.85 (m, 2H), 7.77–7.73 (m, 5H), 7.24 (s, 2H), 7.21 (s, 1H), 4.18 (t, J = 5.9 Hz, 2H), 3.94 (s, 3H), 2.50–2.44 (m, 2H), 1.92–1.83 (m, 4H). ^{13}C NMR (150 MHz, DMSO-d_6) δ 171.63, 155.72, 154.67, 152.34, 151.0 (dd, J = 14.7 Hz, 8.6 Hz), 148.6 (dd, J = 15.5 Hz, 8.8 Hz), 148.48, 147.09, 142.16, 138.11, 136.13 (t, J = 18.2 Hz), 126.66, 118.53, 108.84, 107.32, 105.75, 105.51, 102.32, 68.57, 55.90, 36.01, 28.17, 21.73. HRMS (*m/z*) (ESI): calcd for $C_{26}H_{25}F_3N_5O_5S$ $[M+H]^+$: 576.1523; found: 576.1471.

4.2.3.17. 5-((7-methoxy-4-((2-methoxyphenyl)amino)quinazolin-6-yl)oxy) -*N*-(4-sulfamoylphenyl)pentanamide (**8q**). Yellow solid (yield: 73.1%). ^{1}H NMR (600 MHz, DMSO-d_6) δ 10.31 (s, 1H), 9.13 (s, 1H), 8.28 (s, 1H), 7.83 (s, 1H), 7.77–7.73 (m, 4H), 7.49 (d, J = 7.7 Hz, 1H), 7.25–7.23 (m, 3H), 7.15 (s, 1H), 7.12 (d, J = 8.3 Hz, 1H), 6.99 (t, J = 7.6 Hz, 1H), 4.16 (t, J = 6.3 Hz, 2H), 3.92 (s, 3H), 3.77 (s, 3H), 2.48 (t, J = 7.3 Hz, 2H), 1.89–1.80 (m, 4H). ^{13}C NMR (150 MHz, DMSO-d_6) δ 171.70, 157.68, 154.19, 153.85, 153.22, 148.00, 146.61, 142.21, 138.11, 127.88, 127.38, 126.70, 126.57, 120.21, 118.55, 111.81, 108.75, 107.08, 102.80, 68.40, 55.81, 55.51, 36.04, 28.16, 21.74. HRMS (*m/z*) (ESI): calcd for $C_{27}H_{30}N_5O_6S$ $[M+H]^+$: 552.1911; found: 552.1935.

4.2.3.18. 5-((7-methoxy-4-((4-(trifluoromethyl)phenyl)amino) quinazolin-6- yl)oxy)-*N*-(4-sulfamoylphenyl)pentanamide (**8r**). Yellow solid (yield: 68.4%). ^{1}H NMR (600 MHz, DMSO-d_6) δ 10.28 (s, 1H), 9.70 (s, 1H), 8.55 (s, 1H), 8.11 (d, J = 8.5 Hz, 2H), 7.88 (s, 1H), 7.78–7.73 (m, 6H), 7.24 (s, 2H), 7.23 (s, 1H), 4.21 (t, J = 5.9 Hz, 2H), 3.94 (s, 3H), 2.50–2.45 (m, 2H), 1.92–1.84 (m, 4H). ^{13}C NMR (150 MHz, DMSO-d_6) δ 171.64, 155.95, 154.65, 152.49, 148.47, 147.18, 143.41, 142.17, 138.11, 126.67, 125.63 (d, J = 3.0 Hz), 124.55 (d, J = 270.0 Hz), 122.79 (d, J = 32.0 Hz), 121.44, 118.54, 109.09, 107.29, 102.58, 68.57, 55.91, 36.01, 28.17, 21.74. HRMS (*m/z*) (ESI): calcd for $C_{27}H_{27}F_3N_5O_5S$ $[M+H]^+$: 590.1680; found: 590.1642.

4.2.3.19. 5-((7-methoxy-4-(p-tolylamino)quinazolin-6-yl)oxy)-*N*-(4- sulfamoylphenyl) pentanamide (**8s**). Yellow solid (yield: 66.5%). ^{1}H NMR (600 MHz, DMSO-d_6) δ 10.29 (s, 1H), 9.42 (s, 1H), 8.42 (s, 1H), 7.86 (s, 1H), 7.78–7.73 (m, 4H), 7.65 (d, J = 8.4 Hz, 2H), 7.24 (s, 2H), 7.19 (d, J = 8.3 Hz, 2H), 7.17 (s, 1H), 4.18 (t, J = 5.9 Hz, 2H), 3.93 (s, 3H), 2.50–2.45 (m, 2H), 2.31 (s, 3H), 1.91–1.81 (m, 4H). ^{13}C NMR (150 MHz, DMSO-d_6) δ 171.64, 156.48, 154.28, 152.86, 148.13, 146.59, 142.17, 138.10, 136.76, 132.50, 128.84, 126.66, 122.66, 118.53, 108.79, 107.12, 102.75, 68.49, 55.81, 36.01, 28.15, 21.73, 20.53. HRMS (*m/z*) (ESI): calcd for $C_{27}H_{30}N_5O_5S$ $[M+H]^+$: 536.1962; found: 536.1925.

4.2.3.20. 5-((4-((4-ethylphenyl)amino)-7-methoxyquinazolin-6-yl)oxy)-*N*-(4- sulfamoylphenyl)pentanamide (**8t**). Yellow solid (yield: 65.3%). ^{1}H NMR (600 MHz, DMSO-d_6) δ 10.29 (s, 1H), 9.46 (s, 1H), 8.42 (s, 1H), 7.87 (s, 1H), 7.76 (s, 4H), 7.66 (d, J = 8.0 Hz, 2H), 7.24–7.17 (m, 5H), 4.19 (s, 2H), 3.93 (s, 3H), 2.64–2.58 (m, 2H), 2.48 (d, J = 6.2 Hz, 2H), 1.95–1.80 (m, 4H), 1.22–1.18 (m, 3H). ^{13}C NMR (150 MHz, DMSO-d_6) δ 171.64, 156.51, 154.31, 152.81, 148.14, 146.47, 142.17, 139.01, 138.09, 136.93, 127.63, 126.66, 122.76, 118.53, 108.77, 107.02, 102.79, 68.50, 55.82, 36.00, 28.15, 27.68, 21.73, 15.73. HRMS (*m/z*) (ESI): calcd for $C_{28}H_{32}N_5O_5S$ $[M+H]^+$: 550.2119; found: 550.2077.

4.2.3.21. 5-((7-methoxy-4-(phenylamino)quinazolin-6-yl)oxy)-*N*-(4- sulfamoylphenyl)pentanamide (**8u**). Yellow solid (yield: 63.4%). ^{1}H NMR (600 MHz, DMSO-d_6) δ 10.29 (s, 1H), 9.48 (s, 1H), 8.45 (s, 1H), 7.87 (s, 1H), 7.80–7.75 (m, 6H), 7.39 (t, J = 7.9 Hz, 2H), 7.24 (s, 2H), 7.18 (s, 1H), 7.12 (t, J = 7.4 Hz, 1H), 4.19 (t, J = 5.9 Hz, 2H), 3.93 (s, 3H), 2.48 (t, J = 4.8 Hz, 2H), 1.91–1.81 (m, 4H). ^{13}C NMR (150 MHz, DMSO-d_6) δ 171.64, 156.40, 154.37, 152.79, 148.20, 146.72, 142.17, 139.39, 138.10, 128.40, 126.66, 123.42, 122.50, 118.53, 108.86, 107.15, 102.76, 68.51, 55.83, 36.00, 28.15, 21.73. HRMS (*m/z*) (ESI): calcd for $C_{26}H_{28}N_5O_5S$ $[M+H]^+$: 522.1806; found: 522.1769.

4.2.3.22. 5-((7-methoxy-4-((3-(trifluoromethyl)phenyl)amino) quinazolin-6- yl)oxy)-*N*-(4-sulfamoylphenyl)pentanamide (**8v**). Yellow solid (yield: 61.2%). ^{1}H NMR (600 MHz, DMSO-d_6) δ 10.31 (s, 1H), 9.67 (s, 1H), 8.53 (s, 1H), 8.24–8.21 (m, 2H), 7.86 (s, 1H), 7.80–7.76 (m, 4H), 7.62 (t, J = 7.8 Hz, 1H), 7.44 (d, J = 7.4 Hz, 1H), 7.26–7.22 (m, 3H), 4.20–4.11 (m, 2H), 3.94 (s, 3H), 2.50–2.48 (m, 2H), 1.94–1.89 (m, 2H), 1.85–1.75 (m, 2H). ^{13}C NMR (150 MHz, DMSO-d_6) δ 171.70, 156.05, 154.59, 152.60, 148.45, 147.09, 142.22, 140.50, 138.13, 129.62, 129.23 (d, J = 31.5 Hz), 126.73, 125.48, 124.33 (d, J = 270.0 Hz), 119.31 (d, J = 3.0 Hz), 118.56, 117.86 (d, J = 4.5 Hz), 108.96, 107.31, 102.48, 68.56, 55.93, 36.06, 28.21, 21.79. HRMS (*m/z*) (ESI): calcd for $C_{27}H_{27}F_3N_5O_5S$ $[M+H]^+$: 590.1680; found: 590.1629.

4.2.3.23. 5-((4-((3-chloro-4-((3-fluorobenzyl)oxy)phenyl) amino)-7- methoxyquinazolin-6-yl)oxy)-*N*-(4-sulfamoylphenyl)pentanamide (**8w**). Yellow solid (yield: 69.1%). ^{1}H NMR (600 MHz, DMSO-d_6) δ 10.29 (s, 1H), 9.43 (s, 1H), 8.45 (s, 1H), 7.95 (d, J = 2.6 Hz, 1H), 7.81 (s, 1H), 7.77–7.74 (m, 4H), 7.70 (dd, J = 8.9, 2.5 Hz, 1H), 7.49–7.45 (m, 1H), 7.34–7.31 (m, 2H), 7.27–7.25 (m, 3H), 7.20–7.16 (m, 2H), 5.25 (s, 2H), 4.18 (t, J = 6.2 Hz, 2H), 3.93 (s, 3H), 2.48 (t, J = 7.2 Hz, 2H), 1.92–1.87 (m, 2H), 1.85–1.80 (m, 2H). ^{13}C NMR (150 MHz, DMSO-d_6) δ 171.66, 162.22 (d, J = 242.3 Hz), 156.21, 154.36, 152.83, 149.42, 148.22, 146.82, 142.19, 139.71 (d, J = 7.4 Hz), 138.11, 133.53, 130.57 (d, J = 8.3 Hz), 126.69, 124.03, 123.36 (d, J = 2.6 Hz), 122.20, 121.04, 118.54, 114.71 (d, J = 20.7 Hz), 114.32, 114.06 (d, J = 21.8 Hz), 108.72, 107.28, 102.52, 69.40, 68.49, 55.85, 36.03, 28.18, 21.75. HRMS (*m/z*) (ESI): calcd for $C_{33}H_{32}ClFN_5O_6S$ $[M+H]^+$: 680.1740; found: 680.1670.

4.2.4. Synthesis of 6-amino-4-arylaminoquinazolines (**12a-n**)

Compounds **12a-n** were prepared according to reported procedures [26].

4.2.5. 4-Isothiocyanatobenzenesulfonamide (**14**)

To a solution of sulfanilamide (344 mg, 2.0 mmol) in 10 mL of water, hydrochloric acid (1 mL) was added slowly. After stirred at 0 °C for 5 min, thiophosgen (253 mg, 2.2 mmol) was added. The solution was kept stirring at 0 °C for 2 h and monitored by TLC. After completion of reaction, the reaction mixture was poured into water (50 mL) with stirring to give a white precipitate. The precipitate was purified on silica gel column eluted with DCM/MeOH (50:1 v/v) to give compound 14 (yield 68.6%) as a white solid. ^{1}H NMR (600 MHz, DMSO-d_6) δ 7.86 (d, J = 8.6 Hz, 2H), 7.61 (d, J = 8.6 Hz, 2H), 7.49 (s, 2H).

4.2.6. 4-(2-isothiocyanatoethyl)benzenesulfonamide (**17**)

To a solution of DCC (2.06 g, 10 mmol) in dry THF (30 mL), CS_2 (495 mg, 6.5 mmol) and compound **16** (2.0 g, 4.0 mmol) was added. The reaction was stirred at room temperature overnight and monitored by TLC. After completion of reaction, the solvent was removed under reduced pressure, and then DCM (100 mL) was added, washed with brine three times. The organic phase was dried over Na_2SO_4, and concentrated to dryness under reduced pressure. The residue was subjected to flash column chromatograph over silica gel with DCM/MeOH (100:1 v/v) to give compound 17 (yield 62.0%) as a white solid. ^{1}H NMR (600 MHz, DMSO-d_6) δ 7.79 (d, J = 8.3 Hz, 2H), 7.48 (d, J = 8.3 Hz, 2H), 7.34 (s, 2H), 3.96 (t, J = 6.6 Hz, 2H), 3.04 (t, J = 6.6 Hz, 2H).

*4.2.7. Synthesis of 4-(3-(4-((substituted phenyl)amino)quinazolin-6-yl)thioureido) benzenesulfonamide (**15a-n**) and 4-(2-(3-(4-((substituted phenyl)amino)quinazolin -6-yl)thioureido)ethyl) benzenesulfonamide (**18a-n**)*

To a solution of compound **14** or **17** (0.02 mmol) in anhydrous DMF (5 mL), compound **18a-n** (0.02 mmol) was added and stirred at 60 °C overnight. After completion of reaction, the solvent was removed under reduced pressure. The residue was purified on silica gel column eluted with DCM/MeOH (40:1 v/v) to give the desired products 15a-n and 18a-n.

4.2.7.1. 4-(3-(4-((3-chloro-4-fluorophenyl)amino)quinazolin-6-yl)thioureido) benzenesulfonamide (**15a**). Yellow powder (yield: 71.3%). ^{1}H NMR (600 MHz, DMSO-d_6) δ 11.65 (s, 1H), 11.28 (s, 1H), 11.12 (s, 1H), 8.98 (s, 1H), 8.80 (s, 1H), 8.27 (d, J = 6.1 Hz, 1H), 8.03 (s, 1H), 7.97 (d, J = 7.0 Hz, 1H), 7.86−7.71 (m, 5H), 7.57 (s, 1H), 7.35 (s, 2H). ^{13}C NMR (150 MHz, DMSO-d_6) δ 180.25, 159.60, 155.39 (d, J = 246.2 Hz), 150.38, 142.42, 139.54, 139.40, 136.19, 134.84, 133.97, 126.86, 126.32, 125.51 (d, J = 6.0 Hz), 122.33, 119.96, 119.35 (d, J = 18.0 Hz), 118.67, 117.10 (d, J = 22.5 Hz), 113.78. HRMS (*m/z*) (ESI): calcd for $C_{21}H_{17}ClFN_6O_2S_2$ [M+H]$^+$: 503.0521; found: 503.0466.

4.2.7.2. 4-(3-(4-((3-ethynylphenyl)amino)quinazolin-6-yl)thioureido) benzenesulfonamide (**15b**). Yellow powder (yield: 68.5%). ^{1}H NMR (600 MHz, DMSO-d_6) δ 11.56 (s, 1H), 11.27 (s, 1H), 11.10 (s, 1H), 8.96 (s, 1H), 8.80 (s, 1H), 8.26 (s, 1H), 7.96−7.75 (m, 7H), 7.52−7.35 (m, 4H), 4.32 (s, 1H). ^{13}C NMR (150 MHz, DMSO-d_6) δ 180.27, 159.50, 150.41, 142.44, 139.44, 139.39, 137.12, 136.37, 134.75, 129.76, 129.39, 127.70, 126.32, 125.33, 122.36, 122.16, 120.03, 118.79, 113.87, 82.89, 81.59. HRMS (*m/z*) (ESI): calcd for $C_{23}H_{19}N_6O_2S_2$ [M+H]$^+$: 475.1005; found: 475.0947.

4.2.7.3. 4-(3-(4-((3-(trifluoromethyl)phenyl)amino)quinazolin-6-yl)thioureido) benzenesulfonamide (**15c**). Yellow powder (yield: 75.2%). ^{1}H NMR (600 MHz, DMSO-d_6) δ 11.62 (s, 1H), 11.28 (s, 1H), 11.12 (s, 1H), 8.98 (s, 1H), 8.82 (s, 1H), 8.26 (d, J = 7.4 Hz, 1H), 8.17 (s, 1H), 8.07 (d, J = 5.9 Hz, 1H), 7.97 (d, J = 7.9 Hz, 1H), 7.88−7.69 (m, 6H), 7.35 (s, 2H). ^{13}C NMR (150 MHz, DMSO-d_6) δ 180.29, 159.54, 150.63, 142.46, 139.44, 139.39, 137.87, 137.00, 134.75, 130.12, 129.48 (d, J = 31.8 Hz), 128.40, 126.32, 124.02 (d, J = 270.5 Hz), 122.82, 122.35, 121.03, 120.49, 118.71, 114.00. HRMS (*m/z*) (ESI): calcd for $C_{22}H_{18}F_3N_6O_2S_2$ [M+H]$^+$: 519.0879; found: 519.0813.

4.2.7.4. 4-(3-(4-((4-chloro-3-(trifluoromethyl)phenyl)amino) quinazolin-6-yl) thioureido)benzenesulfonamide (**15d**). Yellow powder (yield: 79.1%). ^{1}H NMR (600 MHz, DMSO-d_6) δ 11.48 (s, 1H), 11.11 (s, 1H), 10.99 (s, 1H), 8.98 (s, 1H), 8.78 (s, 1H), 8.34 (s, 1H), 8.22 (d, J = 7.6 Hz, 1H), 8.14 (d, J = 7.0 Hz, 1H), 7.95 (d, J = 8.1 Hz, 1H), 7.85−7.75 (m, 5H), 7.34 (s, 2H). ^{13}C NMR (150 MHz, DMSO-d_6) δ 180.33, 159.07, 151.00, 142.41, 139.41, 139.23, 136.95, 134.41, 132.08, 132.02, 128.99, 126.89, 126.71 (d, J = 30.8 Hz), 126.26, 122.99, 122.67 (d, J = 271.5 Hz), 122.46, 121.62, 118.53, 114.17. HRMS (*m/z*) (ESI): calcd for $C_{22}H_{17}ClF_3N_6O_2S_2$ [M+H]$^+$: 553.0490; found: 553.0430.

4.2.7.5. 4-(3-(4-((3-bromo-4-fluorophenyl)amino)quinazolin-6-yl)thioureido) benzenesulfonamide (**15e**). Yellow powder (yield: 80.2%). ^{1}H NMR (600 MHz, DMSO-d_6) δ 11.56 (s, 1H), 11.23 (s, 1H), 11.07 (s, 1H), 8.95 (s, 1H), 8.78 (s, 1H), 8.25 (d, J = 7.6 Hz, 1H), 8.14 (s, 1H), 7.95 (d, J = 8.1 Hz, 1H), 7.86−7.76 (m, 5H), 7.53 (s, 1H), 7.34 (s, 2H). ^{13}C NMR (150 MHz, DMSO-d_6) δ 180.27, 159.47, 156.36 (d, J = 243.3 Hz), 150.54, 142.42, 139.43, 139.39, 136.71, 134.67, 134.32, 129.43, 126.30, 126.0 (d, J = 7.8 Hz), 122.36, 120.33, 118.65, 116.81 (d, J = 23.6 Hz), 113.83, 107.69 (d, J = 21.9 Hz). HRMS (*m/z*) (ESI): calcd for $C_{21}H_{17}BrFN_6O_2S_2$ [M+H]$^+$: 547.0016; found: 546.9949.

4.2.7.6. 4-(3-(4-((3-bromophenyl)amino)quinazolin-6-yl)thioureido) benzenesulfonamide (**15f**). Yellow powder (yield: 78.3%). ^{1}H NMR (600 MHz, DMSO-d_6) δ 11.59 (s, 1H), 11.28 (s, 1H), 11.11 (s, 1H), 8.98 (s, 1H), 8.81 (s, 1H), 8.27 (d, J = 8.9 Hz, 1H), 8.03 (s, 1H), 7.97 (d, J = 8.9 Hz, 1H), 7.87 (d, J = 8.6 Hz, 2H), 7.80 (d, J = 8.6 Hz, 2H), 7.74 (d, J = 8.0 Hz, 1H), 7.53 (d, J = 7.9 Hz, 1H), 7.46 (t, J = 8.0 Hz, 1H), 7.34 (s, 2H). ^{13}C NMR (150 MHz, DMSO-d_6) δ 180.25, 159.50, 150.34, 142.41, 139.51, 139.38, 138.39, 136.24, 134.79, 130.77, 129.27, 127.22, 126.29, 123.59, 122.31, 121.25, 119.95, 118.71, 113.85. HRMS (*m/z*) (ESI): calcd for $C_{21}H_{17}BrN_6O_2S_2$ [M+H]$^+$: 529.0111; found: 529.0056.

4.2.7.7. 4-(3-(4-((4-(trifluoromethyl)phenyl)amino)quinazolin-6-yl)thioureido) benzenesulfonamide (**15g**). Yellow powder (yield: 75.0%). ^{1}H NMR (600 MHz, DMSO-d_6) δ 10.33 (s, 1H), 10.30 (s, 1H), 10.11 (s, 1H), 8.69 (s, 1H), 8.58 (s, 1H), 8.15 (d, J = 7.2 Hz, 2H), 7.93 (d, J = 8.4 Hz, 1H), 7.84 (d, J = 8.7 Hz, 1H), 7.80−7.73 (m, 6H), 7.32 (s, 2H). ^{13}C NMR (150 MHz, DMSO-d_6) δ 180.56, 157.31, 153.61, 147.38, 143.01, 142.52, 139.47, 137.36, 132.29, 127.83, 126.17, 125.72 (d, J = 3.5 Hz), 124.47 (d, J = 270.0 Hz), 123.41, 123.19, 121.63, 118.43, 115.24. HRMS (*m/z*) (ESI): calcd for $C_{22}H_{18}F_3N_6O_2S_2$ [M+H]$^+$: 519.0879; found: 519.0811.

4.2.7.8. 4-(3-(4-((3-chloro-2-fluorophenyl)amino)quinazolin-6-yl)thioureido) benzenesulfonamide (**15h**). Yellow powder (yield: 73.5%). ^{1}H NMR (600 MHz, DMSO-d_6) δ 10.31 (s, 1H), 10.27 (s, 1H), 9.95 (s, 1H), 8.51 (s, 1H), 8.44 (d, J = 1.7 Hz, 1H), 7.89 (dd, J = 8.9, 2.0 Hz, 1H), 7.72−7.78 (m, 3H), 7.73 (d, J = 8.7 Hz, 2H), 7.53−7.49 (m, 2H), 7.32 (s, 2H), 7.29 (t, J = 8.1 Hz, 1H). ^{13}C NMR (150 MHz, DMSO-d_6) δ 180.46, 158.09, 154.15, 152.50 (d, J = 247.8 Hz), 147.63, 142.58, 139.42, 137.16, 131.93, 128.08, 128.07 (d, J = 11.8 Hz), 127.53, 126.98, 126.18, 124.97 (d, J = 4.4 Hz), 123.13, 120.20 (d, J = 16.5 Hz), 118.12, 114.79. HRMS (*m/z*) (ESI): calcd for $C_{21}H_{17}ClFN_6O_2S_2$ [M+H]$^+$: 503.0521; found: 503.0463.

4.2.7.9. 4-(3-(4-((3-fluorophenyl)amino)quinazolin-6-yl)thioureido) benzenesulfonamide (**15i**). Yellow powder (yield: 72.0%). ^{1}H NMR (600 MHz, DMSO-d_6) δ 10.33 (s, 1H), 10.32 (s, 1H), 9.91 (s, 1H), 8.66 (s, 1H), 8.54 (s, 1H), 7.95 (d, J = 11.0 Hz, 1H), 7.90 (d, J = 7.5 Hz, 1H), 7.82−7.68 (m, 6H), 7.42 (d, J = 6.9 Hz, 1H), 7.32 (s, 2H), 6.94 (s, 1H). ^{13}C NMR (150 MHz, DMSO-d_6) δ 180.57, 162.00 (d, J = 240.0 Hz), 157.24, 153.86, 147.70, 142.56, 141.13 (d, J = 10.7 Hz), 139.45, 137.15, 132.12, 130.00 (d, J = 9.5 Hz), 128.08, 126.18, 123.17, 118.45, 117.50, 115.20, 109.90 (d, J = 20.9 Hz), 108.59 (d, J = 25.8 Hz). HRMS (*m/z*) (ESI): calcd for $C_{21}H_{18}FN_6O_2S_2$ [M+H]$^+$: 469.0911; found: 469.0857.

4.2.7.10. 4-(3-(4-((3-chlorophenyl)amino)quinazolin-6-yl)thioureido) benzenesulfonamide (**15j**). Yellow powder (yield: 74.7%). ^{1}H NMR (600 MHz, DMSO-d_6) δ 11.48 (s, 1H), 11.21 (s, 1H), 11.05 (s, 1H), 8.96 (s, 1H), 8.80 (s, 1H), 8.25 (d, J = 8.6 Hz, 1H), 7.95 (d, J = 8.9 Hz, 1H), 7.92 (s, 1H), 7.86 (d, J = 8.3 Hz, 2H), 7.80 (d, J = 8.3 Hz, 2H), 7.70 (d, J = 7.8 Hz, 1H), 7.52 (t, J = 8.0 Hz, 1H), 7.39 (d, J = 7.6 Hz, 1H), 7.33 (s, 2H). ^{13}C NMR (150 MHz, DMSO-d_6) δ 180.27, 159.36, 150.54, 142.40, 139.38, 138.41, 136.92, 134.61, 132.90, 130.45, 126.26, 126.17, 124.22, 122.99, 122.35, 120.44, 118.68, 113.91. HRMS (*m/z*) (ESI): calcd for $C_{21}H_{18}ClN_6O_2S_2$ [M+H]$^+$: 485.0616; found: 485.0558.

4.2.7.11. 4-(3-(4-(m-tolylamino)quinazolin-6-yl)thioureido) benzenesulfonamide (**15k**). Yellow powder (yield: 78.6%). ^{1}H NMR (600 MHz, DMSO-d_6) δ 10.27 (s, 1H), 10.23 (s, 1H), 9.72 (s, 1H), 8.58 (s, 1H), 8.53 (s, 1H), 7.86 (d, J = 8.4 Hz, 1H), 7.80−7.73 (m, 5H), 7.66 (s, 2H), 7.33 (s, 2H), 7.27 (t, J = 7.8 Hz, 1H), 6.95 (d, J = 7.1 Hz, 1H), 2.34 (s, 3H). ^{13}C NMR (150 MHz, DMSO-d_6) δ 180.56, 157.51, 154.18, 147.69, 142.61, 139.44, 139.11, 137.66, 136.89, 131.85, 128.35, 128.02, 126.17, 124.47, 123.23, 122.83, 119.56, 118.67, 115.22, 21.25. HRMS (*m/z*) (ESI): calcd for $C_{22}H_{21}N_6O_2S_2$ [M+H]$^+$: 465.1162; found: 465.1104.

4.2.7.12. 4-(3-(4-(p-tolylamino)quinazolin-6-yl)thioureido)benzenesulfonamide (**15l**). Yellow powder (yield: 81.2%). ^{1}H NMR (600 MHz, DMSO-d_6) δ 10.39 (s, 1H), 10.37 (s, 1H), 9.93 (s, 1H), 8.58 (s, 1H), 8.54 (s, 1H), 7.89 (d, J = 8.5 Hz, 1H), 7.80−7.75 (m, 5H), 7.69 (d, J = 8.0 Hz, 2H), 7.33 (s, 2H), 7.21 (d, J = 8.0 Hz, 2H), 2.31 (s, 3H). ^{13}C NMR (150 MHz, DMSO-d_6) δ 180.53, 157.69, 153.75, 146.28, 142.59, 139.40, 137.13, 136.30, 133.21, 132.12, 128.96, 127.02, 126.18, 123.07, 122.70, 118.68, 115.01, 20.58. HRMS (*m/z*) (ESI): calcd for

$C_{22}H_{21}N_6O_2S_2$ $[M+H]^+$: 465.1162; found: 465.1099.

4.2.7.13. 4-(3-(4-((4-ethylphenyl)amino)quinazolin-6-yl)thioureido) benzenesulfonamide (**15m**). Yellow powder (yield: 79.4%). ^{1}H NMR (600 MHz, DMSO-d_6) δ 10.29 (s, 1H), 10.27 (s, 1H), 9.80 (s, 1H), 8.56 (s, 1H), 8.52 (s, 1H), 7.86 (d, J = 8.4 Hz, 1H), 7.80−7.72 (m, 7H), 7.32 (s, 2H), 7.23 (d, J = 8.1 Hz, 2H), 2.62−2.59 (m, 2H), 1.20 (t, J = 7.5 Hz, 3H). ^{13}C NMR (150 MHz, DMSO-d_6) δ 180.55, 162.31, 157.57, 154.06, 147.22, 142.59, 139.42, 136.92, 136.68, 131.90, 127.73, 127.67, 126.16, 123.18, 122.62, 118.67, 115.13, 27.72, 15.78. HRMS (*m/z*) (ESI): calcd for $C_{23}H_{23}N_6O_2S_2$ $[M+H]^+$: 479.1318; found: 479.1256.

4.2.7.14. 4-(3-(4-((3-chloro-4-((3-fluorobenzyl)oxy)phenyl) amino)quinazolin-6- yl)thioureido)benzenesulfonamide (**15n**). Yellow powder (yield: 83.5%). ^{1}H NMR (600 MHz, DMSO-d_6) δ 10.27 (s, 2H), 9.80 (s, 1H), 8.59 (s, 1H), 8.49 (s, 1H), 8.04 (s, 1H), 7.85−7.64 (m, 7H), 7.47−7.18 (m, 7H), 5.25 (s, 2H). ^{13}C NMR (150 MHz, DMSO-d_6) δ 180.56, 162.21 (d, J = 241.8 Hz), 157.32, 154.01, 149.65, 147.46, 142.57, 139.67 (d, J = 6.5 Hz), 139.44, 137.00, 133.21, 131.94, 130.57 (d, J = 7.4 Hz), 127.94, 126.17, 123.96, 123.32, 123.19, 122.15, 121.07, 118.51, 115.05, 114.71 (d, J = 21.2 Hz), 114.35, 114.03 (d, J = 21.6 Hz), 69.40. HRMS (*m/z*) (ESI): calcd for $C_{28}H_{23}ClFN_6O_3S_2$ $[M+H]^+$: 609.0940; found: 609.0873.

4.2.7.15. 4-(2-(3-(4-((3-chloro-4-fluorophenyl)amino)quinazolin-6-yl)thioureido) ethyl)benzenesulfonamide (**18a**). Yellow powder (yield: 78.0%). ^{1}H NMR (600 MHz, DMSO-d_6) δ 9.85 (s, 2H), 8.62 (s, 1H), 8.40 (s, 1H), 8.22 (dd, J = 6.8, 2.6 Hz, 1H), 8.01 (s, 1H), 7.86−7.83 (m, 1H), 7.79−7.76 (m, 4H), 7.46−7.43 (m, 3H), 7.32 (s, 2H), 3.77 (s, 2H), 2.98 (t, J = 7.3 Hz, 2H). ^{13}C NMR (150 MHz, DMSO-d_6) δ 181.11, 157.12, 153.68, 153.29 (d, J = 241.7 Hz), 147.44, 143.51, 142.17, 136.88, 136.58 (d, J = 3.0 Hz), 131.67, 129.14, 128.27, 125.81, 123.38, 122.26 (d, J = 6.8 Hz), 118.82 (d, J = 18.3 Hz), 117.53, 116.61 (d, J = 21.5 Hz), 115.15, 45.24, 34.32. HRMS (*m/z*) (ESI): calcd for $C_{23}H_{21}ClFN_6O_2S_2$ $[M+H]^+$: 531.0834; found: 531.0778.

4.2.7.16. 4-(2-(3-(4-((3-ethynylphenyl)amino)quinazolin-6-yl) thioureido)ethyl) benzenesulfonamide (**18b**). Yellow powder (yield: 82.8%). ^{1}H NMR (600 MHz, DMSO-d_6) δ 9.84 (s, 1H), 9.79 (s, 1H), 8.62 (s, 1H), 8.43 (s, 1H), 8.09 (s, 1H), 8.00 (s, 1H), 7.94 (d, J = 8.2 Hz, 1H), 7.79−7.76 (m, 4H), 7.45 (d, J = 7.6 Hz, 2H), 7.41 (t, J = 7.9 Hz, 1H), 7.33 (s, 2H), 7.23 (d, J = 7.6 Hz, 1H), 4.20 (s, 1H), 3.77 (s, 2H), 2.98 (t, J = 7.3 Hz, 2H). ^{13}C NMR (150 MHz, DMSO-d_6) δ 181.08, 157.24, 153.79, 147.51, 143.53, 142.17, 139.60, 136.79, 131.62, 129.15, 128.96, 128.26, 126.67, 125.82, 124.74, 122.56, 121.78, 117.65, 115.28, 83.53, 80.61, 45.26, 34.33. HRMS (*m/z*) (ESI): calcd for $C_{25}H_{23}N_6O_2S_2$ $[M+H]^+$: 503.1318; found: 503.1274.

4.2.7.17. 4-(2-(3-(4-((3-(trifluoromethyl)phenyl)amino)quinazolin-6-yl) thioureido)ethyl)benzenesulfonamide (**18c**). Yellow powder (yield: 80.5%). ^{1}H NMR (600 MHz, DMSO-d_6) δ 9.97 (s, 1H), 9.86 (s, 1H), 8.65 (s, 1H), 8.45 (s, 1H), 8.34 (s, 1H), 8.26 (d, J = 8.1 Hz, 1H), 8.02 (s, 1H), 7.80−7.76 (m, 4H), 7.63 (t, J = 7.9 Hz, 1H), 7.45 (d, J = 7.5 Hz, 3H), 7.33 (s, 2H), 3.78 (s, 2H), 2.98 (t, J = 7.2 Hz, 2H). ^{13}C NMR (150 MHz, DMSO-d_6) δ 181.12, 157.19, 153.64, 147.53, 143.52, 142.18, 140.23, 136.96, 131.74, 129.66, 129.35, 129.14, 128.31, 125.81, 125.32, 124.25 (d, J = 270.6 Hz), 119.59 (d, J = 3.6 Hz), 117.80 (d, J = 3.9 Hz), 117.57, 115.27, 45.25, 34.32. HRMS (*m/z*) (ESI): calcd for $C_{24}H_{22}F_3N_6O_2S_2$ $[M+H]^+$: 547.1192; found: 547.1122.

4.2.7.18. 4-(2-(3-(4-((4-chloro-3-(trifluoromethyl)phenyl) amino)quinazolin-6- yl)thioureido)ethyl)benzenesulfonamide (**18d**). Yellow powder (yield: 78.9%). ^{1}H NMR (600 MHz, DMSO-d_6) δ 10.03 (s, 1H), 9.87 (s, 1H), 8.67 (s, 1H), 8.48 (d, J = 2.5 Hz, 1H), 8.43 (s, 1H), 8.34 (dd, J = 8.8, 2.1 Hz, 1H), 8.02 (s, 1H), 7.82−7.77 (m, 4H), 7.74 (d, J = 8.8 Hz, 1H), 7.45 (d, J = 7.6 Hz, 2H), 7.32 (s, 2H), 3.77 (s, 2H), 2.98 (t, J = 7.3 Hz, 2H). ^{13}C NMR (150 MHz, DMSO-d_6) δ 181.13, 156.99, 153.47, 147.52, 143.50, 142.18, 139.00, 137.09, 131.84, 131.76, 129.14, 128.35, 126.57, 126.37, 126.26, 125.81, 122.87 (d, J = 271.2 Hz), 120.23 (d, J = 5.4 Hz), 117.43, 115.24, 45.23, 34.31. HRMS (*m/z*) (ESI): calcd for $C_{24}H_{21}ClF_3N_6O_2S_2$ $[M+H]^+$: 581.0803; found: 581.0745.

4.2.7.19. 4-(2-(3-(4-((3-bromo-4-fluorophenyl)amino)quinazolin-6-yl)thioureido) ethyl)benzenesulfonamide (**18e**). Yellow powder (yield: 83.4%). ^{1}H NMR (600 MHz, DMSO-d_6) δ 9.84 (s, 2H), 8.61 (s, 1H), 8.39 (s, 1H), 8.31 (dd, J = 6.4, 2.6 Hz, 1H), 8.00 (s, 1H), 7.92−7.89 (m, 1H), 7.78−7.75 (m, 4H), 7.45 (d, J = 7.7 Hz, 2H), 7.42 (t, J = 8.8 Hz, 1H), 7.32 (s, 2H), 3.77 (s, 2H), 2.98 (t, J = 7.3 Hz, 2H). ^{13}C NMR (150 MHz, DMSO-d_6) δ 181.10, 157.12, 154.44 (d, J = 221.4 Hz), 153.57, 147.44, 143.52, 142.17, 136.82 (d, J = 2.9 Hz), 131.67, 129.14, 128.26, 126.15, 125.81, 125.73, 122.96 (d, J = 6.9 Hz), 117.53, 116.37 (d, J = 22.8 Hz), 115.14, 107.24 (d, J = 21.6 Hz), 45.25, 34.32. HRMS (*m/z*) (ESI): calcd for $C_{23}H_{21}BrFN_6O_2S_2$ $[M+H]^+$: 575.0329; found: 575.0257.

4.2.7.20. 4-(2-(3-(4-((3-bromophenyl)amino)quinazolin-6-yl) thioureido)ethyl) benzenesulfonamide (**18f**). Yellow powder (yield: 78.5%). ^{1}H NMR (600 MHz, DMSO-d_6) δ 9.84 (s, 1H), 9.82 (s, 1H), 8.64 (s, 1H), 8.42 (s, 1H), 8.24 (s, 1H), 8.01 (s, 1H), 7.92 (d, J = 8.2 Hz, 1H), 7.80−7.75 (m, 4H), 7.45 (d, J = 7.7 Hz, 2H), 7.36 (t, J = 8.0 Hz, 1H), 7.32−7.29 (m, 3H), 3.77 (s, 2H), 2.98 (t, J = 7.3 Hz, 2H). ^{13}C NMR (150 MHz, DMSO-d_6) δ 181.07, 157.11, 153.68, 147.49, 143.50, 142.17, 141.04, 136.86, 131.67, 130.42, 129.13, 128.27, 125.92, 125.80, 123.99, 121.21, 120.54, 117.56, 115.28, 45.25, 34.32. HRMS (*m/z*) (ESI): calcd for $C_{23}H_{22}BrN_6O_2S_2$ $[M+H]^+$: 557.0424; found: 557.0347.

4.2.7.21. 4-(2-(3-(4-((4-(trifluoromethyl)phenyl)amino)quinazolin-6-yl) thioureido)ethyl)benzenesulfonamide (**18g**). Yellow powder (yield: 76.8%). ^{1}H NMR (600 MHz, DMSO-d_6) δ 10.01 (s, 1H), 9.87 (s, 1H), 8.66 (s, 1H), 8.46 (s, 1H), 8.17 (d, J = 8.4 Hz, 2H), 8.02 (s, 1H), 7.83−7.75 (m, 6H), 7.45 (d, J = 7.4 Hz, 2H), 7.32 (s, 2H), 3.77 (s, 2H), 2.98 (t, J = 7.1 Hz, 2H). ^{13}C NMR (150 MHz, DMSO-d_6) δ 181.07, 157.15, 153.57, 147.60, 143.51, 143.16, 142.18, 137.00, 131.75, 129.14, 128.30, 125.81, 125.71 (d, J = 3.6 Hz), 124.51 (d, J = 269.7 Hz), 123.12 (d, J = 31.8 Hz), 121.44, 117.52, 115.39, 45.26, 34.32. HRMS (*m/z*) (ESI): calcd for $C_{24}H_{22}F_3N_6O_2S_2$ $[M+H]^+$: 547.1192; found: 547.1116.

4.2.7.22. 4-(2-(3-(4-((3-chloro-2-fluorophenyl)amino)quinazolin-6-yl)thioureido) ethyl)benzenesulfonamide (**18h**). Yellow powder (yield: 82.0%). ^{1}H NMR (600 MHz, DMSO-d_6) δ 9.91 (s, 1H), 9.85 (s, 1H), 8.50 (s, 1H), 8.34 (s, 1H), 8.02 (s, 1H), 7.81−7.75 (m, 4H), 7.54−7.45 (m, 4H), 7.32 (s, 2H), 7.29 (t, J = 8.0 Hz, 1H), 3.77 (s, 2H), 2.99 (t, J = 7.3 Hz, 2H). ^{13}C NMR (150 MHz, DMSO-d_6) δ 181.12, 158.00, 153.95, 152.46 (d, J = 247.9 Hz), 147.38, 143.52, 142.18, 136.99, 131.58, 129.15, 128.11 (d, J = 12.0 Hz), 127.45, 126.91, 125.81, 125.73, 124.95 (d, J = 4.4 Hz), 120.20 (d, J = 16.4 Hz), 117.31, 114.88, 45.20, 34.28. HRMS (*m/z*) (ESI): calcd for $C_{23}H_{21}ClFN_6O_2S_2$ $[M+H]^+$: 531.0834; found: 531.0761.

4.2.7.23. 4-(2-(3-(4-((3-fluorophenyl)amino)quinazolin-6-yl) thioureido)ethyl) benzenesulfonamide (**18i**). Yellow powder (yield: 84.5%). ^{1}H NMR (600 MHz, DMSO-d_6) δ 9.85 (s, 2H), 8.64 (s, 1H), 8.43 (s, 1H), 8.00 (s, 1H), 7.96 (d, J = 11.9 Hz, 1H), 7.81−7.75 (m, 4H), 7.69 (d, J = 8.1 Hz, 1H), 7.46−7.40 (m, 3H), 7.32 (s, 2H), 6.94 (t, J = 8.3 Hz, 1H), 3.77 (s, 2H), 2.98 (t, J = 7.2 Hz, 2H). ^{13}C NMR (150 MHz, DMSO-d_6) δ 181.09, 161.99 (d, J = 239.3 Hz), 157.15, 153.69, 147.52, 143.51, 142.17, 141.19 (d, J = 11.0 Hz), 136.86, 131.67, 129.98 (d, J = 9.6 Hz), 129.13, 128.27, 125.81, 117.58, 117.40 (d, J = 2.3 Hz), 115.30, 109.76 (d, J = 21.0 Hz), 108.42 (d, J = 26.0 Hz), 45.24, 34.32. HRMS (*m/z*) (ESI): calcd for $C_{23}H_{22}FN_6O_2S_2$ $[M+H]^+$: 497.1224; found: 497.1175.

4.2.7.24. 4-(2-(3-(4-((3-chlorophenyl)amino)quinazolin-6-yl) thioureido)ethyl) benzenesulfonamide (**18j**). Yellow powder (yield: 85.2%). ^{1}H NMR (600 MHz, DMSO-d_6) δ 9.83 (s, 2H), 8.64 (s, 1H), 8.43 (s, 1H), 8.13 (s, 1H), 8.01 (s, 1H), 7.86 (d, J = 8.3 Hz, 1H), 7.80−7.75 (m, 4H), 7.45 (d, J = 7.5 Hz, 2H), 7.42 (t, J = 8.1 Hz, 1H), 7.32 (s, 2H), 7.16 (d, J = 7.9 Hz, 1H), 3.77 (s, 2H), 2.98 (t, J = 7.2 Hz, 2H). ^{13}C NMR (150 MHz, DMSO-d_6) δ 181.08, 157.13, 153.69, 147.51, 143.51, 142.17, 140.91, 136.87, 132.76, 131.68, 130.11, 129.13, 128.27,

125.81, 123.02, 121.17, 120.13, 117.58, 115.28, 45.25, 34.32. HRMS (*m/z*) (ESI): calcd for $C_{23}H_{22}ClN_6O_2S_2$ $[M+H]^+$: 513.0929; found: 513.0861.

4.2.7.25. 4-(2-(3-(4-(m-tolylamino)quinazolin-6-yl)thioureido) ethyl) benzenesulfonamide (**18k**). Yellow powder (yield: 80.7%). ^{1}H NMR (600 MHz, DMSO-d_6) δ 9.82 (s, 1H), 9.68 (s, 1H), 8.57 (s, 1H), 8.43 (s, 1H), 7.99 (s, 1H), 7.79–7.74 (m, 4H), 7.67 (s, 2H), 7.46 (d, J = 6.7 Hz, 2H), 7.34 (s, 2H), 7.27 (t, J = 7.6 Hz, 1H), 6.95 (d, J = 7.2 Hz, 1H), 3.78 (s, 2H), 2.99 (s, 2H), 2.34 (s, 3H). ^{13}C NMR (150 MHz, DMSO-d_6) δ 181.08, 157.43, 154.02, 147.49, 143.56, 142.18, 139.17, 137.64, 136.59, 131.48, 129.17, 128.34, 128.19, 125.84, 124.40, 122.74, 119.48, 117.86, 115.34, 45.29, 34.37, 21.26. HRMS (*m/z*) (ESI): calcd for $C_{24}H_{25}N_6O_2S_2$ $[M+H]^+$: 493.1475; found: 493.1408.

4.2.7.26. 4-(2-(3-(4-(p-tolylamino)quinazolin-6-yl)thioureido) ethyl) benzenesulfonamide (**18l**). Yellow powder (yield: 79.5%). ^{1}H NMR (600 MHz, DMSO-d_6) δ 9.81 (s, 1H), 9.68 (s, 1H), 8.53 (s, 1H), 8.40 (s, 1H), 7.97 (s, 1H), 7.79–7.71 (m, 6H), 7.45 (d, J = 6.7 Hz, 2H), 7.33 (s, 2H), 7.19 (d, J = 7.9 Hz, 2H), 3.76 (s, 2H), 2.98 (s, 2H), 2.30 (s, 3H). ^{13}C NMR (150 MHz, DMSO-d_6) δ 181.07, 157.41, 154.06, 147.47, 143.55, 142.17, 136.64, 136.50, 132.73, 131.42, 129.15, 128.90, 128.17, 125.82, 122.36, 117.87, 115.29, 45.28, 34.36, 20.56. HRMS (*m/z*) (ESI): calcd for $C_{24}H_{25}N_6O_2S_2$ $[M+H]^+$: 493.1475; found: 493.1411.

4.2.7.27. 4-(2-(3-(4-((4-ethylphenyl)amino)quinazolin-6-yl)thioureido)ethyl) benzenesulfonamide (**18m**). Yellow powder (yield: 83.6%). ^{1}H NMR (600 MHz, DMSO-d_6) δ 9.81 (s, 1H), 9.69 (s, 1H), 8.53 (s, 1H), 8.40 (s, 1H), 7.97 (s, 1H), 7.78 (d, J = 8.2 Hz, 2H), 7.75–7.72 (m, 4H), 7.45 (d, J = 7.5 Hz, 2H), 7.32 (s, 2H), 7.22 (d, J = 8.3 Hz, 2H), 3.76 (s, 2H), 2.98 (t, J = 7.2 Hz, 2H), 2.62–2.58 (m, 2H), 1.20 (t, J = 7.6 Hz, 3H). ^{13}C NMR (150 MHz, DMSO-d_6) δ 181.07, 157.43, 154.06, 147.48, 143.54, 142.17, 139.20, 136.82, 136.51, 131.42, 129.14, 128.16, 127.70, 125.81, 122.45, 117.87, 115.29, 45.28, 34.35, 27.71, 15.79. HRMS (*m/z*) (ESI): calcd for $C_{25}H_{27}N_6O_2S_2$ $[M+H]^+$: 507.1631; found: 507.1563.

4.2.7.28. 4-(2-(3-(4-((3-chloro-4-((3-fluorobenzyl)oxy)phenyl) amino)quinazolin -6-yl)thioureido)ethyl)benzenesulfonamide (**18n**). Yellow powder (yield: 82.2%). ^{1}H NMR (600 MHz, DMSO-d_6) δ 9.82 (s, 1H), 9.73 (s, 1H), 8.57 (s, 1H), 8.37 (s, 1H), 8.05 (s, 1H), 7.98 (s, 1H), 7.78–7.70 (m, 5H), 7.47–7.39 (m, 3H), 7.38–7.32 (m, 4H), 7.27 (d, J = 8.8 Hz, 1H), 7.18 (t, J = 7.3 Hz, 1H), 5.25 (s, 2H), 3.77 (s, 2H), 2.98 (s, 2H). ^{13}C NMR (150 MHz, DMSO-d_6) δ 181.09, 162.21 (d, J = 242.1 Hz), 157.20, 153.89, 149.56, 147.39, 143.52, 142.17, 139.68 (d, J = 7.4 Hz), 136.68, 133.32, 131.51, 130.58 (d, J = 8.3 Hz), 129.14, 128.19, 125.81, 123.80, 123.33 (d, J = 2.3 Hz), 122.01, 121.04, 117.67, 115.15, 114.71 (d, J = 20.7 Hz), 114.36, 114.03 (d, J = 21.8 Hz), 69.40, 45.25, 34.33. HRMS (*m/z*) (ESI): calcd for $C_{30}H_{27}ClFN_6O_3S_2$ $[M+H]^+$: 637.1253; found: 637.1208.

4.3. Cell lines and cell growth inhibition assay

The NSCLC cell lines A549, H1975, human epidermoid carcinoma cell line A431 and normal human liver cells LO2 in this study were purchased from China Life Science College (Shanghai, PRC). Roswell Park Memorial Institute (RPMI) 1640 medium, Culture medium Dulbecco's modified Eagle medium (DMEM), fetal bovine serum (FBS), phosphate buffered saline (PBS, pH 7.2), and Antibiotic-Antimycotic came from KeyGen Biotech Company (China). Cells were grown in the medium supplemented with 10% FBS, 100 units per mL penicillin and 100 g/mL streptomycin in a humidified atmosphere of normoxia (20% O_2, 75% N_2 and 5% CO_2) or hypoxia (1% O_2, 94% N_2 and 5% CO_2) at 37 °C. Then, the compounds were dissolved in DMSO and diluted with medium to various concentrations (the final concentration of DMSO was less than 0.4%). After being incubated at 37 °C for 72 h, cells were stained with 3-(4,5-dimethyl-2-thiazolyl)-2,5-diphenyl-2Htetrazolium bromide (MTT, 5 mg/mL) for another 4 h, and then dissolved with 150 μL of DMSO. The O.D. value was read at 570/630 nm enzyme labeling instrument. The IC_{50} values were calculated by SPSS software after three parallel experiments.

4.4. EGFR kinase inhibition assay

The EGFR proteins ($EGFR^{WT}$ and $EGFR^{T790M}$) were purchased from Carna Bioscience. The HTRF KinEASE-TK kit (Cat#62TK0PEB) was from Cisbio. All the other chemicals were from Sigma. The EGFR kinase assays were performed in 384-well plate (Corning 3676, low volume, black, NBS), using Cisbio HTRF KinEASE-TK kit. The assay buffer contained 50 mM HEPES (Ph 7.0), 0.02% NaN_3, 0.01% BSA, 0.1 mM Orthovanadate, 10 mM $MgCl_2$, 2.5 mM DTT and 6.25 nM SEB. EGFR kinases was first incubated with compounds for 2 h respectively, then ATP/Peptide substrate mixture was added to initiate the reaction. After 30 min reaction at room temperature, the detection reagents were added. The TR-FRET signal was measured on PerkinElmer Envision using excitation 320 nm and emission 615 nm/665 nm. The data was analyzed using Graph Pad Prism (Version 6.0) software after three parallel experiments.

4.5. CA inhibitory assay

Enzyme inhibition assays of CA (CAII and CAIX) were carried out as per previous reported method [27]. This assay spectrophotometrically measured the p-nitrophenol, a yellow colored product which is formed by the hydrolysis of p-nitrophenyl acetate (4-PNA) catalyzed by CA. Absorbance was measured at 400 nm with the help of UV/visible spectrophotometer (Shimadzu UV2600) equipped with temperature regulator. The absorption data was analyzed with the help of Graph Pad Prism (Version 6.0) and the IC_{50} values for tested compounds were determined.

4.6. Apoptosis assay

Apoptosis was detected by flow cytometry with annexin V/PI staining. H1975 cells were grown in each well of six-well plates at the density of 5×10^4 cells per mL in the RPMI 1640 medium with 10% FBS to the final volume of 2 mL. The plates were incubated overnight and treated with test compounds at the indicated concentration for 24 h. Then, cells were harvested and washed twice with ice-cold PBS, and then suspended in the annexin-binding buffer at a concentration of 5×10^5 cells per mL. Cells were then incubated with 5 mL of annexin V-FITC and 5 mL of PI for 30 min at room temperature in the dark. The samples were analyzed for fluorescence with a flow cytometer (FACS Calibur, BD Biosciences).

4.7. Cell cycle measurement

H1975 cells with good vitality were transferred into six-well plates and cultured overnight at 37 °C. Then, compounds at the indicated concentration were incubated with cells for 24 h. All adherent and floating cells were collected and washed twice with PBS. Then, the cells were fixed with 70% EtOH at 4 °C for 24 h. After that, fixed cells were washed with PBS. After being centrifuged, cells were stained with 50 μg/mL propidium iodide solution containing 100 μg/mL RNase at 37 °C for 0.5 h. The samples (at least 1×10^4 cells) were measured by flow cytometry (FAC Scan, Becton Dickenson) using Cell Quest software and recording propidium iodide (PI) in the FL2 channel.

4.8. Wound healing assays

H1975 cells were seeded in each well of 6-well plates and cultured. After the cells were attached to the wall, drew a straight

line along the ruler with a yellow pipette tip and washed twice with PBS and the serum-free medium was added. Then, cells were incubated with 0.5 and 1.0 μM of **8v,** respectively. A negative control was treated only with culture medium. After 24 h of incubation, the scratches were visualized and photographed using an inverted microscope to observe cellular migration through the wounds. The area of the wound was precisely circled along the edge of the cell scratch for quantitative analysis. The migration rate = (0 h wound area − 48 h wound area)/0 h wound area.

4.9. Western blot analysis

Western blot analysis was performed as our described before [28]. Briefly, H1975 cells were treated with **8v** at the indicated concentration (2 or 5 μM) for 24 h under the normoxic or hypoxic conditions. Untreated cells were used as a negative control. Cells treated with gefitinib and acetazolamide were used as positive controls. After for 24 h, cells were collected, centrifuged, and washed twice with ice-cold PBS. The pellet was then resuspended in lysis buffer. After the cells were lysed on ice for 30 min, lysates were centrifuged at 20 000 g at 4 °C for 10 min. The protein concentration in the supernatant was detected by the BCA protein assay reagents. Equal amounts of protein per line were separated by 12% SDS polyacrylamide gel electrophoresis and transferred to PVDF Hybond-P membranes (GE Healthcare). The membranes were incubated with 5% skim milk in Tris-buffered saline with Tween 20 (TBST) buffer for 1 h and then the membranes were gently rotated overnight at 4 °C. The membranes were then incubated with primary antibodies against EGFR, p-EGFR, AKT, p-AKT, ERK, p-ERK, CAIX or HIF-1α overnight at 4 °C. The membranes were next incubated with peroxidase labeled secondary antibodies for 2 h. Then, all the membranes were washed with TBST four times for 20 min and the protein blots were detected by a chemiluminescence reagent (Thermo Fischer Scientifics Ltd). The X-ray films were developed with developer and fixed with fixer solution.

4.10. Molecular docking

The $EGFR^{WT}$, $EGFR^{T790M}$ and CAIX protein structures used for the docking studies were retrieved from the RCSB Protein Data Bank (rcsb.org) (PDB IDs: 2ITY ($EGFR^{WT}$), 2JIU ($EGFR^{T790M}$) and 3IAI (CAIX)), which were chosen as the template to elucidate the binding mode of compound **8v**. The receptor protein structures and ligand coordinates were prepared as follows: 1) the native ligand and water molecules were removed from the crystal structure; 2) all hydrogen atoms were added to each protein and ligand to be docked and each coordinate file of protein and ligand was generated as PDBQT file using AutoDockTools-1.5.6 (The Scripps Research Institute, La Jolla, California, USA); 3) A grid box for binding site covered the catalytic site of the protein or 40 Å in the three dimensions for allosteric binding site and centered at the geometric center of the protein. Docking results were manually inspected, and the binding poses with the most favorable binding affinity and meaningful geometry were visualized with PyMOL.

Declaration of competing interest

The authors declare that they have no known competing financial interests or personal relationships that could have appeared to influence the work reported in this paper.

Acknowledgment

The authors are grateful to Jiangsu Province Hi-tech Key Laboratory for Biomedical Research for financial aids to this research.

Appendix A. Supplementary data

Supplementary data to this article can be found online at https://doi.org/10.1016/j.ejmech.2021.113300.

References

[1] (a) M. Cheng, X.F. Yu, K. Lu, L. Xie, L. Wang, F.Y. Meng, X.R. Han, X. Chen, J. Liu, Y. Xiong, J. Jin, Discovery of potent and selective epidermal growth factor receptor (EGFR) bifunctional small-molecule degraders, J. Med. Chem. 63 (2020) 1216–1232;
(b) P. Bhatia, V. Sharma, O. Alam, A. Manaithiya, P. Alam, Kahksha, M.T. Alam, M. Imran, Novel quinazoline-based EGFR kinase inhibitors: a review focussing on SAR and molecular docking studies (2015-2019),, Eur. J. Med. Chem. 204 (2020) 112640;
(c) C. Bailly, Contemporary challenges in the design of topoisomerase II inhibitors for cancer chemotherapy, Chem. Rev. 112 (2012) 3611–3640.

[2] (a) A. Anighoro, J. Bajorath, G. Rastelli, Polypharmacology: challenges and opportunities in drug discovery, J. Med. Chem. 57 (2014) 7874–7887;
(b) E. Shang, Y. Yuan, X. Chen, Y. Liu, J. Pei, L. Lai, De novo design of multitarget ligands with an iterative fragment-growing strategy, J. Chem. Inf. Model. 54 (2014) 1235–1241.

[3] H.M. Hesham, D.S. Lasheen, K.A.M. Abouzid, Chimeric HDAC inhibitors: comprehensive review on the HDAC-based strategies developed to combat cancer, Med. Res. Rev. 38 (2018) 2058–2109.

[4] (a) R.G. Fu, Y. Sun, W.B. Sheng, D.F. Liao, Designing multi-targeted agents: an emerging anticancer drug discovery paradigm, Eur. J. Med. Chem. 136 (2017) 195–211;
(b) E. Proschak, H. Stark, D. Merk, Polypharmacology by design: a medicinal chemist's perspective on multitargeting compounds, J. Med. Chem. 62 (2019) 420–444;
(c) H.M. Alkahtani, A.N. Abdalla, A.J. Obaidullah, M.M. Alanazi, A.A. Almehizia, M.G. Alanazi, A.Y. Ahmed, O.I. Alwassil, H.W. Darwish, A.A.M. Abdel-Aziz, A.S. El-Azab, Synthesis, cytotoxic evaluation, and molecular docking studies of novel quinazoline derivatives with benzenesulfonamide and anilide tails: dual inhibitors of EGFR/HER2, Bioorg. Chem. 95 (2020) 103461;
(d) , in: T.J. Anastasio (Ed.), Computational and Experimental Approaches in Multi-Target Pharmacology, Front. Pharmacol., vol. 8, 2017, p. 443.

[5] (a) J.R. Goffin, K. Zbuk, Epidermal growth factor receptor: pathway, therapies, and pipeline, Clin. Therapeut. 35 (2013) 1282–1303;
(b) S. Peters, S. Zimmermann, A.A. Adjei, Oral epidermal growth factor receptor tyrosine kinase inhibitors for the treatment of non-small cell lung cancer: comparative pharmacokinetics and drug-drug interactions, Canc. Treat Rev. 40 (2014) 917–926;
(c) D.A. Reardon, P.Y. Wen, I.K. Mellinghoff, Targeted molecular therapies against epidermal growth factor receptor: past experiences and challenges, Neuro Oncol. 16 (2014) viii7–viii13.

[6] (a) D.S. Krause, R.A. Van Etten, Tyrosine kinases as targets for cancer therapy, N. Engl, J. Med. 353 (2005) 172–187;
(b) S.V. Sharma, D.W. Bell, J. Settleman, D.A. Haber, Epidermal growth factor receptor mutations in lung cancer, Nat. Rev. Canc. 7 (2007) 169–181;
(c) M. Nadeem Abbas, S. Kausar, F. Wang, Y. Zhao, H. Cui, Advances in targeting the epidermal growth factor receptor pathway by synthetic products and its regulation by epigenetic modulators as a therapy for glioblastoma, Cells 8 (2019) 350–361.

[7] (a) N. Tebbutt, M.W. Pedersen, T.G. Johns, Targeting the ERBB family in cancer: couples therapy, Nat. Rev. Canc. 13 (2013) 663–673;
(b) J. Zhang, P.L. Yang, N.S. Gray, Targeting cancer with small molecule kinase inhibitors, Nat. Rev. Canc. 9 (2009) 28–39.

[8] (a) T.S. Mok, Y.L. Wu, S. Thongprasert, C.H. Yang, D.T. Chu, N. Saijo, P. Sunpaweravong, B.H. Han, B. Margono, Y. Ichinose, Y. Nishiwaki, Y. Ohe, J.J. Yang, B. Chewaskulyong, H.Y. Jiang, E.L. Duffield, C.L. Watkins, A.A. Armour, M. Fukuoka, Gefitinib or carboplatin-paclitaxel in pulmonary adenocarcinoma, N. Engl, J. Med. 316 (2009) 947–957;
(b) N.M. Andrews Wright, G.D. Goss, Third-generation epidermal growth factor receptor tyrosine kinase inhibitors for the treatment of non-small cell lung cancer, Transl. Lung Cancer Res. 8 (2019) S247–S264.

[9] H.A. Yu, M.E. Arcila, N. Rekhtman, C.S. Sima, M.F. Zakowski, W. Pao, M.G. Kris, V.A. Miller, M. Ladanyi, G.J. Riely, Analysis of tumor specimens at the time of acquired resistance to EGFR-TKI therapy in 155 patients with EGFR-mutant lung cancers, Clin. Canc. Res. 19 (2013) 2240–2247.

[10] (a) A.O. Walter, R.T.T. Sjin, H.J. Haringsma, K. Ohashi, J. Sun, K. Lee, A. Dubrovskiy, M. Labenski, Z. Zhu, Z. Wang, M. Sheets, T. St Martin, R. Karp, D. van Kalken, P. Chaturvedi, D. Niu, M. Nacht, R.C. Petter, W. Westlin, K. Lin, S. Jaw-Tsai, M. Raponi, T. Van Dyke, J. Etter, Z. Weaver, W. Pao, J. Singh, A.D. Simmons, T.C. Harding, A. Allen, Discovery of a mutant-selective covalent inhibitor of EGFR that overcomes T790M-mediated resistance in NSCLC, Canc. Discov. 3 (2013) 1404–1415;
(b) R.A. Ward, M.J. Anderton, S. Ashton, P.A. Bethel, M. Box, S. Butterworth, N. Colclough, C.G. Chorley, C. Chuaqui, D.A.E. Cross, L.A. Dakin, J.É. Debreczeni, C. Eberlein, M.R.V. Finlay, G.B. Hill, M. Grist, T.C.M. Klinowska, C. Lane, S. Martin, J.P. Orme, P. Smith, F. Wang, M.J. Waring, Structure- and reactivity-based development of covalent inhibitors of the activating and gatekeeper

mutant forms of the epidermal growth factor receptor (EGFR), J. Med. Chem. 56 (2013) 7025–7048.

[11] (a) K.S. Thress, C.P. Paweletz, E. Felip, B.C. Cho, D. Stetson, B. Dougherty, Z. Lai, A. Markovets, A. Vivancos, Y. Kuang, D. Ercan, S.E. Matthews, M. Cantarini, J.C. Barrett, P.A. Janne, G.R. Oxnard, Acquired EGFR C797S mutation mediates resistance to AZD9291 in non-small cell lung cancer harboring EGFR T790M, Nat. Med. 21 (2015) 560–562;
(b) H. Patel, R. Pawara, A. Ansari, S. Surana, Recent updates on third generation EGFR inhibitors and emergence of fourth generation EGFR inhibitors to combat C797S resistance, Eur. J. Med. Chem. 142 (2017) 32–47.

[12] (a) Q. Li, T. Zhang, S. Li, L. Tong, J. Li, Z. Su, F. Feng, D. Sun, Y. Tong, X. Wang, Z. Zhao, L. Zhu, J. Ding, H. Li, H. Xie, Y. Xu, Discovery of potent and noncovalent reversible EGFR kinase inhibitors of EGFR(L858R/T790M/C797S), ACS Med. Chem. Lett. 10 (2019) 869–873;
(b) J. Shen, T. Zhang, S.J. Zhu, M. Sun, L. Tong, M. Lai, R. Zhang, W. Xu, R. Wu, J. Ding, C.H. Yun, H. Xie, X. Lu, K. Ding, Structure-based design of 5-methylpyrimidopyridone derivatives as new wild-type sparing inhibitors of the epidermal growth factor receptor triple mutant (EGFR(L858R/T790M/C797S)), J. Med. Chem. 62 (2019) 7302–7308;
(c) H. Park, H.Y. Jung, S. Mah, S. Hong, Discovery of EGF receptor inhibitors that are selective for the d746-750/T790M/C797S mutant through structure-based de novo design, Angew. Chem. 129 (2017) 7742–7746.

[13] (a) J. Folkman, What is the evidence that tumors are angiogenesis dependent? J. Natl. Cancer Inst. 82 (1990) 4–6;
(b) C.G. Qian, J.C. Yu, Y.L. Chen, Q.Y. Hu, X.Z. Xiao, W.J. Sun, C. Wang, P.J. Feng, Q.D. Shen, Z. Gu, Light-activated hypoxia-responsive nanocarriers for enhanced anticancer therapy, Adv. Mater. 28 (2016) 3313–3320.

[14] (a) S. Pennacchietti, P. Michieli, M. Galluzzo, M. Mazzone, S. Giordano, P.M. Comoglio, Hypoxia promotes invasive growth by transcriptional activation of the met protooncogene, Canc. Cell 3 (2003) 347–361;
(b) Q. Chang, I. Jurisica, T. Do, D.W. Hedley, Hypoxia predicts aggressive growth and spontaneous metastasis formation from orthotopically grown primary xenografts of human pancreatic cancer, Canc. Res. 71 (2011) 3110–3120;
(c) S.H. Kwak, T.N. Stephenson, H.E. Lee, Y. Ge, H. Lee, S.M. Min, J.H. Kim, D.Y. Kwon, Y.M. Lee, J. Hong, Evaluation of manassantin a tetrahydrofuran core region analogues and cooperative therapeutic effects with EGFR inhibition, J. Med. Chem. 63 (2020) 6821–6833.

[15] (a) J.T. Andring, W. Dohle, C. Tu, B.V.L. Potter, R. McKenna, 3,17β-Bis-sulfamoyloxy-2-methoxyestra-1,3,5(10)-triene and nonsteroidal sulfamate derivatives inhibit carbonic anhydrase IX: structure-activity optimization for isoform selectivity, J. Med. Chem. 62 (2019) 2202–2212;
(b) A. Angeli, E. Trallori, M. Ferraroni, L.D.C. Mannelli, C. Ghelardini, C.T. Supuran, Discovery of new 2,5-disubstituted 1,3-selenazoles as selective human carbonic anhydrase IX inhibitors with potent anti-tumor activity, Eur. J. Med. Chem. 157 (2018) 1214–1222.

[16] (a) Y. Lu, Y. Liu, S. Oeck, P.M. Glazer, Hypoxia promotes resistance to EGFR inhibition in NSCLC cells via the histone demethylases, LSD1 and PLU-1, Mol. Canc. Res. 16 (2018) 1458–1469;
(b) A. Franovic, L. Gunaratnam, K. Smith, I. Robert, D. Patten, S. Lee, Translational up-Regulation of the EGFR by tumor hypoxia provides a nonmutational explanation for its overexpression in human cancer, Proc. Natl. Acad. Sci. U.S.A. 104 (2007) 13092–13097.

[17] D.E.B. Swinson, K.J. O'Byrne, Interactions between hypoxia and epidermal growth factor receptor in non-small-cell lung cancer, Clin. Lung Canc. 7 (2006) 250–256.

[18] (a) D. Das, J. Hong, Recent advancements of 4-aminoquinazoline derivatives as kinase inhibitors and their applications in medicinal chemistry, Eur. J. Med. Chem. 170 (2019) 55–72;
(b) S. Shagufta, I. Ahmad, An insight into the therapeutic potential of quinazoline derivatives as anticancer agents, Med. Chem. Comm 8 (2017) 871–885;
(c) R.S.M. Ismail, N.S.M. Ismail, S. Abuserii, D.A. Abou El Ella, Recent advances in 4-aminoquinazoline based scaffold derivatives targeting EGFR kinases as anticancer agents, Futur. J. Pharm. Sci. 2 (2016) 9–19.

[19] (a) D.A.A. El Ella, M.M. Ghorab, H.I. Heiba, A.M. Soliman, Synthesis of some new thiazolopyrane and thiazolopyranopyrimidine derivatives bearing a sulfonamide moiety for evaluation as anticancer and radiosensitizing agents, Med. Chem. Res. 21 (2012) 2395–2407;
(b) S. Hao, X. Cheng, X. Wang, R. An, H. Xu, M. Guo, C. Li, Y. Wang, Z. Hou, C. Guo, Design, synthesis and biological evaluation of novel carbohydrate-based sulfonamide derivatives as antitumor agents, Bioorg. Chem. 104 (2020) 104237.

[20] (a) Y. Ju, J. Wu, X. Yuan, L. Zhao, G. Zhang, C. Li, R. Qiao, Design and evaluation of potent EGFR inhibitors through the incorporation of macrocyclic polyamine moieties into the 4-anilinoquinazoline scaffold, J. Med. Chem. 61 (2018) 11372–11383;
(b) R.D. Li, X. Zhang, Q.Y. Li, Z.M. Ge, R.T. Li, Novel EGFR inhibitors prepared by combination of dithiocarbamic acid esters and 4-anilinoquinazolines, Bioorg. Med. Chem. Lett 21 (2011) 3637–3640.

[21] R.L. McKee, R.W. Bost, p-Substituted phenyl isothiocyanates and some related thioureas, J. Am. Chem. Soc. 68 (1946) 2506–2507.

[22] Y. Chen, L. Yang, H. Qiao, Z. Cheng, J. Xie, W. Zhou, X. Huang, Y. Jiang, B. Yu, W. Zhao, Discovery of new thieno [3,2-d]pyrimidine derivatives targeting $EGFR^{L858R/T790M}$ NSCLCs by the conformation constrained strategy, Eur. J. Med. Chem. 199 (2020) 112388.

[23] M.M. Ghorab, M.S. Alsaid, A.M. Soliman, F.A. Ragab, VEGFR-2 inhibitors and apoptosis inducers: synthesis and molecular design of new benzo [g] quinazolin bearing benzenesulfonamide moiety, J. Enzym. Inhib. Med. Chem. 32 (2017) 893–907.

[24] C.H. Yun, T.J. Boggon, Y. Li, M.S. Woo, H. Greulich, M. Meyerson, M.J. Eck, Structures of lung cancer-derived EGFR mutants and inhibitor complexes: mechanism of activation and insights into differential inhibitor sensitivity, Canc. Cell 11 (2007) 217–227.

[25] C.H. Yun, K.E. Mengwasser, A.V. Toms, M.S. Woo, H. Greulich, K.K. Wong, M. Meyerson, M.J. Eck, The T790M mutation in EGFR kinase causes drug resistance by increasing the affinity for ATP, Proc. Natl. Acad. Sci. U.S.A. 105 (2008) 2070–2075.

[26] R.S.M. Ismail, S.M. Abou-Seri, W.M. Eldehna, N.S.M. Ismail, S.M. Elgazwi, H.A. Ghabbour, M.S. Ahmed, F.T. Halaweish, D.A. Abou El Ella, Novel series of 6-(2-substitutedacetamido)-4-anilinoquinazolines as EGFR-ERK signal transduction inhibitors in MCF-7 breast cancer cells, Eur. J. Med. Chem. 155 (2018) 782–796.

[27] (a) F. Shamsi, P. Hasan, A. Queen, A. Hussain, P. Khan, B. Zeya, H.M. King, S. Rana, J. Garrison, M.F. Alajmi, M.M.A. Rizvi, M. Zahid, M.I. Hassan, M. Abid, Synthesis and SAR studies of novel 1,2,4-oxadiazole-sulfonamide based compounds as potential anticancer agents for colorectal cancer therapy, Bioorg. Chem. 98 (2020) 103754;
(b) M.N. Peerzada, P. Khan, K. Ahmad, M.I. Hassan, A. Azam, Synthesis, characterization and biological evaluation of tertiary sulfonamide derivatives of pyridyl-indole based heteroaryl chalcone as potential carbonic anhydrase IX inhibitors and anticancer agents, Eur. J. Med. Chem. 155 (2018) 13–23.

[28] (a) Z.K. Liu, M. Wang, H.S. Wang, L. Fang, S.H. Gou, Platinum-based modification of styrylbenzylsulfones as multifunctional antitumor agents: targeting the RAS/RAF pathway, enhancing antitumor activity, and overcoming multidrug resistance, J. Med. Chem. 63 (2020) 186–204;
(b) B. Zhang, X.C. Huang, H.S. Wang, S.H. Gou, Promoting antitumor efficacy by suppressing hypoxia via nano self-assembly of two irinotecan-based dual drug conjugates having a HIF-1a inhibitor, J. Mater. Chem. B 7 (2019) 5352–5362.